ACS OMEGA

Open Access

http://pubs.acs.org/journal/acsodf

Article

New Thiophenyl-pyrazolyl-thiazole Hybrids as DHFR Inhibitors: Design, Synthesis, Antimicrobial Evaluation, Molecular Modeling, and Biodistribution Studies

Dina H. Dawood,* Manal M. Sayed, Sally T. K. Tohamy, and Eman S. Nossier

Cite This: *ACS Omega* 2023, 8, 39250−39268

Read Online

ACCESS | Metrics & More | Article Recommendations | Supporting Information

ABSTRACT: The antibiotic resistance problems constitute a considerable threat to human health worldwide; thus, the discovery of new antimicrobial candidates to conquer this issue is an imperative requirement. From this view, new thiophenyl-pyrazolyl-thiazole hybrids **3**−**10** were synthesized and screened for their antibacterial efficiency versus Gram − and Gram + bacterial strains compared to the reference drug amoxicillin. It was noticed that the new hybrids displayed significant antibacterial efficacy versus Gram − bacteria, especially against *Pseudomonas aeruginosa*. Also, all the screened candidates demonstrated a noticeable antifungal effect against *Candida albicans* (MICs = 3.9−125 μg/mL) relative to fluconazole (MIC = 250 μg/mL). Moreover, the new hybrids were investigated for their antituberculosis potency against *Mycobacterium tuberculosis* (RCMB 010126). Derivatives **4c**, **6b**, **8b**, **9b**, and **10b** demonstrated prominent antituberculosis efficiency (MICs = 0.12−1.95 μg/mL) compared with the reference drug isoniazid (MIC = 0.12 μg/mL). The latter derivatives were further assessed for their inhibitory potency versus *M. tuberculosis* DHFR enzyme. The compounds **4c**, **6b** and **10b** presented a remarkable suppression effect with IC_{50} values of 4.21, 5.70, and 10.59 μM, respectively, compared to that of trimethoprim (IC_{50} = 6.23 μM). Furthermore, biodistribution profile using radiolabeling way revealed a perceived uptake of ^{131}I-compound **6b** into infection induced models. The docking study for the new hybrids **4c**, **6b**, **8b**, **9b** and **10b** was performed to illustrate the various binding modes with *Mtb* DHFR enzyme. In silico ADMET studies for the most potent inhibitors **4c**, **6b** and **10b** were also accomplished to predict their pharmacokinetic and physicochemical features.

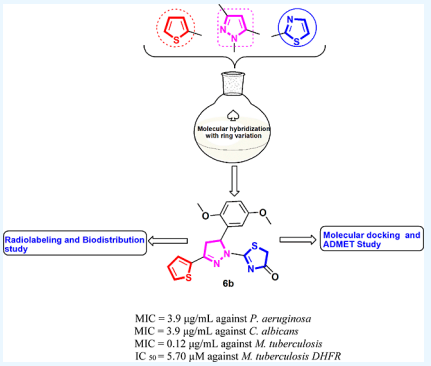

1. INTRODUCTION

Antimicrobial-resistant infections are deemed to be a significant threat to human health in this century,[1,2] and this is attributed to the alteration of the characteristics of the infectious microbes and incorrect diagnosis as well as the misuse of the antimicrobial agents.[3] It is predicated that the drug−resistant microbes will increase the mortality in the coming years.[4] Hence, the discovery of novel antimicrobial agents that overcome the increasing risks of the drug−resistant infectious microbes is an urgent requirement.

The antifolates are a class of therapeutics that have received extensive attention for their antimicrobial efficiency[5] targeting *Mycobacterium tuberculosis* (*Mtb*).[6−9] Antifolates suppress the dihydrofolate reductase enzyme (DHFR), which plays a crucial role in the folate metabolism by stimulation of the reduction of dihydrofolate to tetrahydrofolate utilizing nicotinamide adenine dinucleotide phosphate as a coenzyme factor in many pathogens inclusive *Mtb*.[6−10] Tetrahydrofolate is a pivotal precursor for the synthesis of thymidylate, purine nucleotides, and various amino acids that are essential for DNA, RNA, and protein synthesis.[5,11,12] Therefore, the suppression of DHFR enzyme results in an imbalance in the synthetic pathway of active thymidylate, causing the disruption of DNA replication, which in turn leads to cell death.[13] Lately, DHFR structures of organisms like *Mtb* have been disclosed.[6−10] So, the discovery of new molecules as DHFR inhibitors especially against *Mtb* is a promising goal in the treatment of tuberculosis.

Thiophene scaffold has drawn attention in the medicinal field due to its significant variation in the pharmacological activities,[14−17] mostly as antimicrobial agents.[6,18−21] The thiophene moiety was found to be the basic skeleton of various antibiotics such as cephalothin and cefoxitin and different antifungal agents such as sertaconazole and tioconazole[22] (Figure 1). Moreover, thiophene-pyrazolone hybrids **I** and **II** were reported as potent antibacterial agents versus *Pseudomonas aeruginosa*, *Bacillus subtilis*, and *Staphylococcus aureus* strains and antifungal agents versus *C. albicans* and *A. fumigates*[23] (Figure 2). Furthermore, Asiri and Khan[24]

Received: July 3, 2023
Accepted: September 25, 2023
Published: October 13, 2023

https://doi.org/10.1021/acsomega.3c04736
ACS Omega 2023, 8, 39250−39268

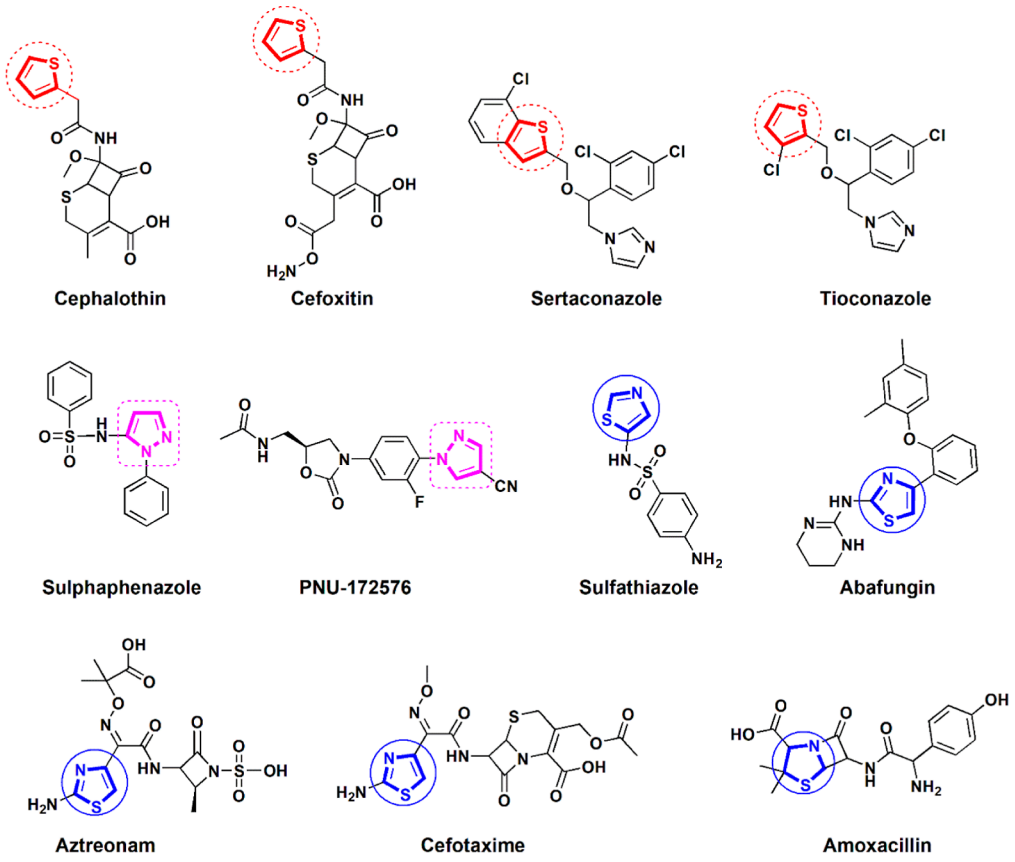

Figure 1. Various antimicrobial drugs containing thiophene, pyrazole, and thiazole moieties.

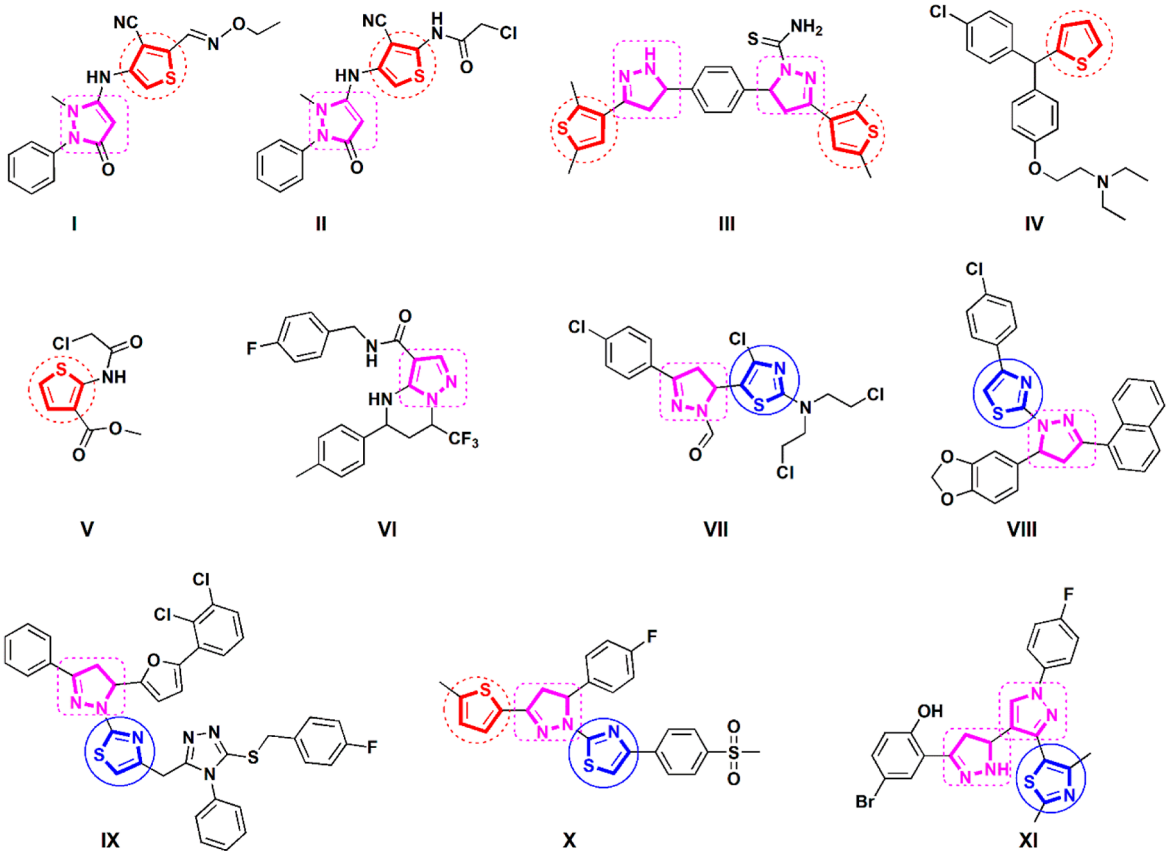

Figure 2. Various antimicrobial compounds bearing thiophene, pyrazole, and thiazole moieties.

https://doi.org/10.1021/acsomega.3c04736
ACS Omega 2023, 8, 39250−39268

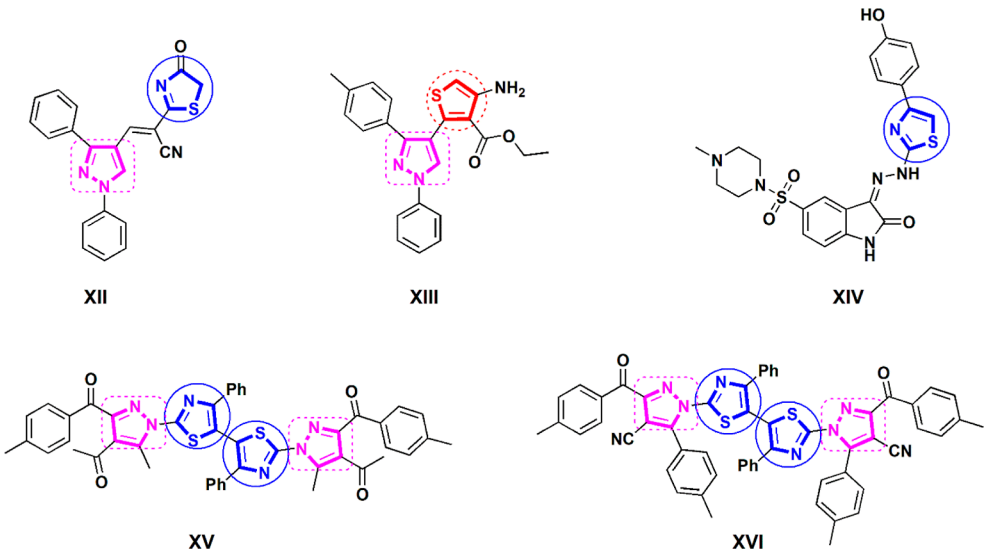

Figure 3. Some thiophene, pyrazole, and thiazole derivatives as potent DHFR inhibitors.

showed that the pyrazoline derivative conjugated with thiophene moiety **III** revealed significant antibacterial potency against *Escherichia coli* and *S. aureus* (Figure 2). In addition, the pyrazole motif is an integral portion of some antibiotics like sulphaphenazole and PNU-172576[25] (Figure 1). Moreover, various thiophene and pyrazole based derivatives **IV**–**VI** exhibited remarkable antituberculosis efficiency[26−28] (Figure 2). The thiazole moiety is a core structural component of varied bioactive molecules including antimicrobial drugs like sulfathiazole and antifungal drugs such as abafungin[29,30] (Figure 1). Moreover, various market antibiotics bear a thiazole ring such as aztreonam, cefotaxime, and amoxicillin[30−32] (Figure 1). Additionally, thiazolylpyrazoline hybrids **VII**–**XI** have been introduced by many research groups as potent antibacterial, antifungal, and antituberculosis agents[33−37] (Figure 2).

Lately, Mohamed et al.[38] detected that the hybridization of pyrazole scaffold with thiazole or thiophene subunits such as compounds **XII** and **XIII** has a noticeable effect on the suppression of DHFR enzyme. Furthermore, the thiazole derivative **XIV** demonstrated prominent efficacy as a DHFR inhibitor.[39] In addition, bis-pyrazolyl thiazole candidates **XV** and **XVI** were identified by Ibrahim et al. as eminent DHFR suppressors (Figure 3).[40]

Molecular hybridization has stood out as a substantial approach in the discovery of new bioactive entities, which was attained via the conjugation of various nuclei in a single structure to enhance the biological efficacy. The design strategy for the synthesizing and screening of the new thiophenyl-pyrazolyl-thiazole hybrids **3**–**10** as antimicrobial agents targeting DHFR enzyme relied on the above-mentioned facts and considering the efficiency of thiophene scaffold as well as the pyrazole and thiazole moieties as antimicrobial candidates and DHFR inhibitors (Figure 4).

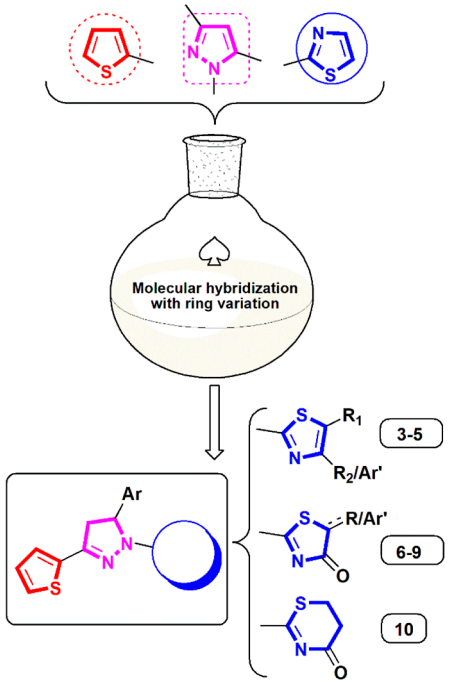

Figure 4. Design strategy of the new thiophenyl-pyrazolyl-thiazole hybrids **3**–**10**.

2. RESULTS AND DISCUSSION

2.1. Chemistry. The synthetic procedures for the preparation of various thiophenyl-pyrazolyl-thiazole hybrids are depicted in Schemes 1 and 2. Thiopenylpyrazole-1-carbothioamide derivatives **2a,b** were synthesized via condensation of chalcones **1a,b** with thiosemicabazide in ethanol containing potassium hydroxide as a basic medium. The compounds **2a,b** were utilized as beneficial intermediates for the synthesis of varied bioactive heterocyclic derivatives. The ^{1}H NMR spectrum of **2b** detected a set of three doublets of doublet at 2.96, 3.85, and 6.02 ppm due to the methylene and methine protons of the pyrazoline moiety, respectively, and two singlets at 3.64 and 3.79 ppm assignable to the dimethoxy groups and two D_2O exchangeable singlets at 7.61 and 8.03 ppm, attributed to the NH_2 functional group. Furthermore, the heterocyclization of thiophenylpyrazole-1-carbothioamide derivatives **2a,b** with diversified halogenated ketones, viz., chloroacetone, phenacyl bromide, and 4-bromophenacyl bromide in absolute ethanol in the presence of anhydrous sodium acetate conferred the diverse substituted thiazoles **3a,b** and **4a**–**c**, respectively. In an identical way, the reaction of the

https://doi.org/10.1021/acsomega.3c04736
ACS Omega 2023, 8, 39250−39268

Scheme 1. Synthesis of New Thiophenyl-pyrazolyl-thiazole Hybrids 3−5[a]

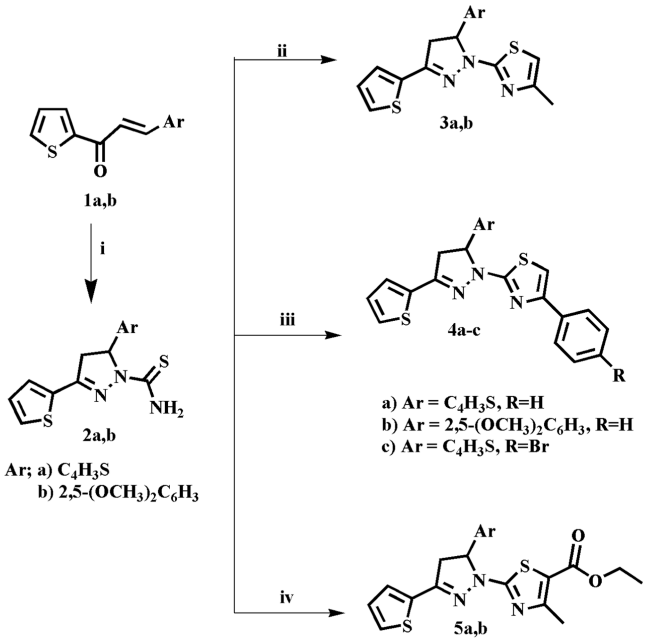

[a]Reagents and conditions: (i) $NH_2CSNHNH_2$, EtOH, KOH. reflux for 8 h; (ii) H_3CCOCH_2Cl. CH_3COONa, EtOH, reflux for 6−8 h; (iii) $PhCOCH_2Br$/4-$BrPhCOCH_2Br$, CH_3COONa, EtOH, reflux for 6−8 h; (iv) $CH_3COCH(Cl)COOC_2H_5$, CH_3COONa, EtOH, reflux for 6−8 h.

intermediates **2a,b** with ethyl-2-chloroacetoacetate gave 4-methylthiazole-5-ethylcarboxylates **5a,b**, respectively. The ^{1}H NMR spectra of the new thiophenylpyrazolyl-thiazole hybrids **3−10** represented three doublets of doublet at the zones of 2.95−3.70, 3.81−4.14, and 5.60−6.27 ppm, referring to the methylene (H_4, H_4') and methine protons (H_5) of the pyrazoline moiety, respectively. Furthermore, ^{1}H NMR spectra of **3a,b** and **4a−c** disclosed a singlet signal at the zone of 6.44−7.44 ppm, referring to H_5 of the thiazole ring. The noticeable features of ^{1}H NMR spectra of **5a,b** are the apparition of triplet and quartet signals at 1.26 and 4.17−4.19 ppm, respectively, assignable to the ethyl protons. ^{13}C NMR spectra of the new thiophenyl-pyrazolyl-thiazole hybrids detected signals at 43.42−44.29 ppm and 59.48−60.29 ppm for the methylene and methine carbons of the pyrazoline moiety, respectively, along with a signal related to the methyl carbon of the thiazole revealed at 17.81 ppm for compound **3b**. On the other hand, a significant increment in the number of signals was noticed in the aromatic zone at 105.18−164.66 ppm, due to the presence of the phenyl ring for compound **4a**. Otherwise, signals representing the ethyl carbon were detected at 14.72−14.73 and 60.63−60.69 ppm, besides the carbonyl ester at 164.87−164.97 ppm for compounds **5a,b** (Scheme 1).

The thiazolidinone derivatives **6a,b** were synthesized via reaction of thiophenylpyrazole-1-carbothioamide derivatives **2a,b** with ethyl bromoacetate in ethanolic solution in the existence of piperidine as a catalyst. However, refluxing the thiophenylpyrazole-1-carbothioamide derivatives **2a,b** with ethyl-2-bromopropionate in ethanolic solution employing anhydrous sodium acetate conferred the corresponding 5-methylthiazolidinones **7a,b**. The ^{1}H NMR spectra of **6a,b** demonstrated the methylene protons of the thiazolidinone as a singlet signal at 3.95−3.96 ppm, whereas ^{1}H NMR spectra of **7a,b** displayed quartet signals at 4.16−4.18 ppm due to the methine protons of the thiazolidinone. The ^{13}C NMR spectrum of **7a** demonstrated two signals related to the methine carbon of the thiazole and the carbonyl group at 49.49 and 189.91 ppm, respectively. Moreover, the multicomponent condensation of the intermediates **2a,b** with ethyl bromoacetate and substituted aromatic aldehydes in glacial acetic acid via employing an anhydrous sodium acetate afforded the corresponding 5-substituted benzylidene thiazolidinone derivatives **8a−d**. Also, 5-indolin-2-one thiazolidinone derivatives **9a,b** were achieved via refluxing of the intermediates **2a,b** with ethyl bromoacetate and isatin under the same reaction conditions. ^{1}H NMR spectra of **8a−d** exhibited the existence of a singlet signal at 7.65−7.86 ppm attributed to the olefinic protons. Moreover, the ^{13}C NMR spectrum of **8c** displayed three signals at 56.04, 56.60, and 179.34 ppm, referring to the two methoxy and carbonyl groups, respectively, alongside the increment of the number of the signals in the aromatic zone at 113.37−170.45 ppm, indicating the presence of the phenyl moiety. However, ^{1}H NMR spectra of **9a,b** revealed D_2O exchangeable singlets at 11.17 and 11.20 pm assignable to the NH groups of indolin-2-one moiety. The ^{13}C NMR spectrum of compound **9a** revealed the existence of two signals at 173.13 and 179.33 due to two carbonyl groups. The reaction of thiopenylpyrazole-1-carbothioamide derivatives **2a,b** with 3-bromopropanoic acid yielded the corresponding 1,3-thiazin-4-one derivatives **10a,b**. ^{1}H NMR spectra of **10a,b** presented multiplet signals at 3.18−3.25 ppm due to two methylene groups of the thiazine rings (Scheme 2). The IR and mass spectra of the new thiophenylpyrazolyl-thiazole hybrids were proportionate with their structures.

2.2. Antimicrobial Activities. *2.2.1. Antibacterial Efficiency.* In vitro estimation of the antibacterial efficacy of the new thiophenyl-pyrazolyl-thiazole hybrids was accomplished utilizing broth microdilution assay versus two Gram − bacterial strains, viz., *P. aeruginosa* (ATCC 29853) and *E. coli* (ATCC 25922) and two Gram + bacterial strains, viz., *S. aureus* (ATCC 25923) and *B. subtilis* (ATCC 9372), comparative to the reference drug amoxicillin. The minimum inhibitory concentration (MIC, μg/mL) and minimum bactericidal concentration (MBC, μg/mL) for the screened derivatives are depicted in Tables 1 and 2.

The antibacterial assessment displayed the significant sensitivity of the Gram − bacteria *P. aeruginosa* toward all of the screened candidates except for compounds (**3a**, **5a,** and **7a**) with MICs values ranging from 3.9 to 125 μg/mL compared to amoxicillin with MIC > 500 μg/mL. It has been noticed that the 5-(2,5-dimethoxyphenyl)-3-thiophenylpyrazolyl-thiazolone hybrid **6b** demonstrated the most prominent antibacterial efficiency with MIC = 3.9 μg/mL against *P. aeruginosa*. On the other hand, compounds **3b** and **4b** were approximately 32-fold more efficient as antibacterial agents against *P. aeruginosa* (MIC = 15.625 μg/mL) than amoxicillin, while compounds **4c**, **5b**, **8a**, **8c**, **9a,** and **10a** were almost 16-fold more efficacious (MIC = 31.25 μg/mL) than amoxicillin.

However, the rest of the investigated hybrids represented 8−4-fold more antibacterial effectiveness (MICs = 62.25−125 μg/mL) than that exerted by amoxicillin. Otherwise, most of the investigated analogs exhibited reasonable antibacterial efficacy against *E. coli* with MICs of 62.5−125 μg/mL relative to amoxicillin (MIC = 62.5 μg/mL). The pyrazole-1-carbothioamide derivative **2b** is equipotent to amoxicillin

https://doi.org/10.1021/acsomega.3c04736
ACS Omega 2023, 8, 39250−39268

Scheme 2. Synthesis of New Thiophenyl-pyrazolyl-thiazolone/thiazinone Hybrids 6−10[a]

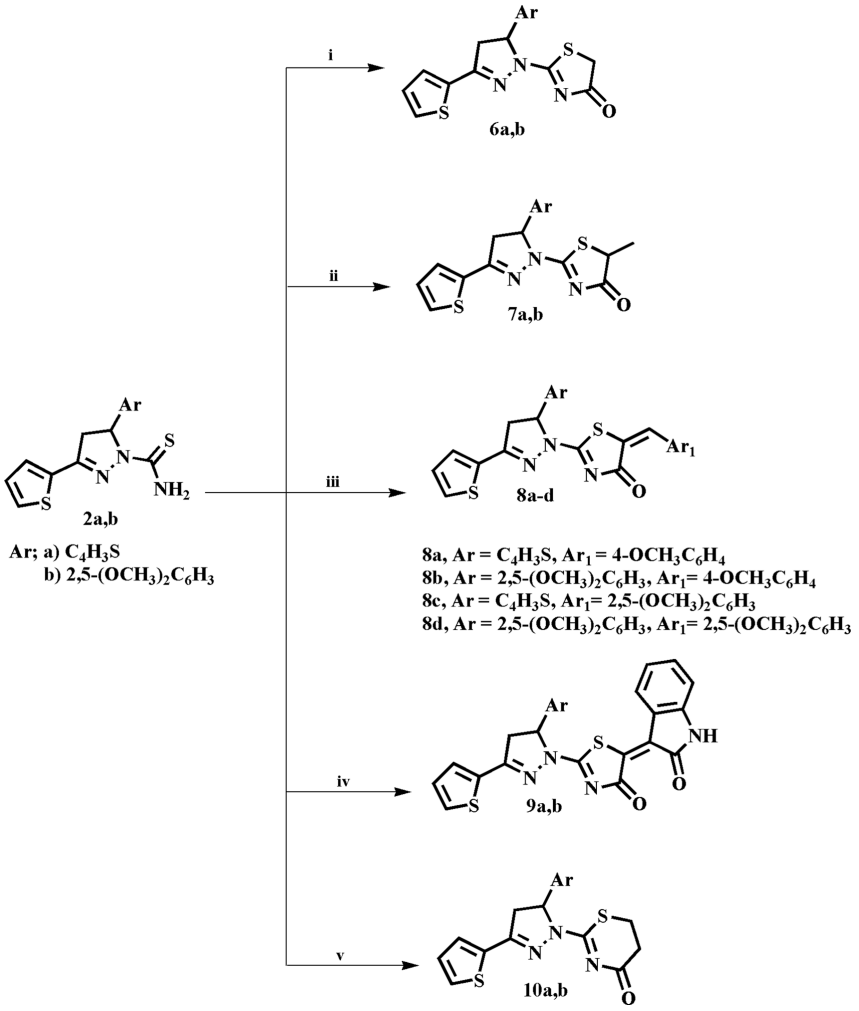

[a]Reagents and conditions: (i) $CH_3CH_2COOCH_2Br$, EtOH, piperidine, reflux for 3 h; (ii) $BrCH(CH_3)COOC_2H_5$, CH_3COONa, EtOH, reflux for 8−10 h; (iii) $CH_3CH_2COOCH_2Br$, ArCHO, CH_3COONa, AcOH, reflux for 3−5 h; (iv) $CH_3CH_2COOCH_2Br$, isatin, CH_3COONa, AcOH, reflux for 3−5 h; (v) $BrCH_2CH_2COOH$, CH_3COONa, AcOH, reflux for 6 h.

with an MIC value of 62.5 μg/mL. It was distinctly observed that the majority of the screened hybrids were 2-fold less efficient compared to amoxicillin against *E. coli* with MIC = 125 μg/mL. On the contrary, the examined hybrids appeared to be inactive as antibacterial candidates versus Gram + bacterial strain *S. aureus,* with MICs ranging from 62.5 to > 500 μg/mL compared to amoxicillin (MIC = 7.8 μg/mL). The antibacterial efficiency was slightly enhanced against *B. subtilis* with MICs = 3.9−250 μg/mL compared to amoxicillin (MIC = 31.25 μg/mL). It is worth mentioning that the conjugation of 3,5-dithiophenylpyrazolyl scaffold with 4-phenylthiazole **4a** or 4-methylthiazole-5-ethyl carboxylate **5a** revealed 2−8-fold more antibacterial efficiency against *B. subtilis* (MICs = 15.625 and 3.9 μg/mL, respectively) than that achieved by amoxicillin (MIC = 31.25 μg/mL). However, the other screened hybrids disclosed 2−8-fold less potency (MICs = 62.5−250 μg/mL) than amoxicillin against *B. subtilis*.

It could be deduced from the attained results that most of the investigated analogs **4a**, **4c**, **5b**, **6a**, **6b**, **7b**, **8d**, **9a**, **9b**, **10a,** and **10b** displayed bactericidal effects against *P. aeruginosa* as the ratio of MBC/MIC ≤ 4. The other derivatives demonstrate bacteriostatic potential (Table 2). It was noticeably apparent that the new thiophenyl-pyrazolyl-thiazole hybrids displayed significant antibacterial efficacy versus Gram − bacteria especially against *P. aeruginosa* more than Gram + bacteria.

A summarized discussion of the structure−activity relationships against *P. aeruginosa* displayed that 5-(2,5-dimethoxyphenyl)-3-(thiophenyl)pyrazolyl-carbothioamide derivative **2b** revealed significant antibacterial efficiency (MIC = 62.25 μg/mL). The hybridization of 5-(2,5-dimethoxyphenyl)-3-(thiophen-2-yl) pyrazolyl scaffold with 4-methyl/phenylthiazole such as compounds **3b** and **4b** enhanced the antibacterial efficacy (MIC = 15.625 μg/mL). On the other hand, the activity declined 2-fold upon the substitution of the thiazole ring with an ethyl carboxylate group as compound **5b** (MIC = 31.25 μg/mL). Otherwise, a remarkable antibacterial effect was achieved via the hybridization of the 5-(2,5-dimethoxyphenyl)-3-(thiophen-2-yl) pyrazolyl scaffold with the unsubstituted thiazolidinone ring **6b** (MIC = 3.9 μg/mL), while a noticeable decrease in the antibacterial efficiency was detected by the introduction of 5-methyl group **7b** to the thiazolidinone moiety (MIC = 125 μg/mL), but it is still more efficient than amoxicillin. Conversely, the replacement of the methyl group with substituted benzylidene groups **8b** and **8d** significantly enhanced the antibacterial effect (MIC = 62.25 μg/mL). Furthermore, the remarkable antibacterial efficiency was

https://doi.org/10.1021/acsomega.3c04736
ACS Omega 2023, 8, 39250−39268

Table 1. Minimum Inhibitory Concentration (μg/mL) of the New Thiophenyl-pyrazolyl-thiazole Hybrids against Tested Microbes

compound	Gram-negative bacteria		Gram-positive bacteria		fungi
	E. coli (ATCC25922)	P. aeruginosa (ATCC 29853)	S. aureus (ATCC 25923)	B. subtilis (ATCC 9372)	C. albicans (ATCC 10231)
2b	62.5	62.25	250	125	62.5
3a	500	>500	250	62.5	125
3b	125	15.625	250	125	31.25
4a	125	125	250	15.625	125
4b	125	15.625	250	250	62.5
4c	>500	31.25	62.5	125	3.9
5a	>500	>500	62.5	3.9	125
5b	125	31.25	62.5	125	62.5
6a	125	62.5	250	125	62.5
6b	125	3.9	62.5	125	3.9
7a	125	>500	>500	125	62.5
7b	125	125	250	125	62.5
8a	125	31.25	250	125	62.5
8b	>500	62.25	62.5	62.5	31.25
8c	125	31.25	62.5	125	31.25
8d	125	62.25	62.5	125	62.5
9a	125	31.25	62.5	125	125
9b	125	62.25	62.5	125	31.25
10a	125	31.25	125	62.5	62.5
10b	125	62.25	250	62.5	15.625
amoxicillin	62.5	>500	7.8	31.25	
fluconazole					250

Table 2. Ratios (MBC/MIC or MFC/MIC) of the Thiophenyl-pyrazolyl-thiazole Hybrids and Positive Controls against *P. aeruginosa* and *C. albicans*

compound	Gram-negative bacteria			fungi		
	P. aeruginosa (ATCC 29853)			C. albicans (ATCC 10231)		
	MIC	MBC	ratio	MIC	MFC	ratio
2b	62.25	500	8	62.5	250	4
3a	>500	>500	>1	125	>500	>4
3b	15.625	125	8	31.25	250	8
4a	125	500	4	125	500	4
4b	15.625	250	16	62.5	500	8
4c	31.25	125	4	3.9	31.25	8
5a	>500	>500	>1	125	500	4
5b	31.25	62.25	2	62.5	125	2
6a	62.5	250	4	62.5	250	4
6b	3.9	15.625	4	3.9	15.625	4
7a	>500	>500	>1	62.5	250	4
7b	125	250	2	62.5	500	8
8a	31.25	250	8	62.5	125	2
8b	62.25	500	8	31.25	125	4
8c	31.25	250	8	31.25	62.25	2
8d	62.25	125	2	62.5	125	2
9a	31.25	62.25	2	125	250	2
9b	62.25	125	2	31.25	500	16
10a	31.25	125	4	62.5	250	4
10b	62.25	250	4	15.625	31.25	2
amoxicillin	>500	>500	>1			
fluconazole				250	250	1

conserved upon replacement of the substituted benzylidene group with indolinone ring **9b** (MIC = 62.25 μg/mL); in a similar way, the conjugation of the 5-(2,5-dimethoxyphenyl)-3-(thiophen-2-yl) pyrazolyl scaffold with thiazinone ring **10b** promoted the antibacterial efficacy (MIC = 62.25 μg/mL). On the other hand, the antibacterial efficiency was reduced by the 3,5-di(thiophen-2-yl)pyrazolyl analogs but was still more effective than amoxicillin except for compounds **4c**, **8a, 8c, 9a,** and **10a,** which exerted eminent antibacterial potency (Figure 5).

2.2.2. Antifungal Efficiency. The new thiophenyl-pyrazolyl-thiazole hybrids were assessed for their antifungal efficiency against *Candida albicans* (ATCC 10231) utilizing fluconazole as a reference drug (Table 1). All the screened candidates represented outstanding antifungal efficacy with MICs (3.9−125 μg/mL) relative to fluconazole (MIC = 250 μg/mL). Among the investigated compounds, **4c** and **6b** disclosed eminent antifungal efficiency (MIC = 3.9 μg/mL) compared to fluconazole (MIC = 250 μg/mL). However, the other analogs demonstrated 16−2-fold more antifungal efficacy (MICs = 15.625−125 μg/mL) than fluconazole (MIC = 250 μg/mL). Furthermore, a fungicidal behavior was exerted by all screened candidates except compounds **3a**, **3b**, **4b**, **4c**, **7b,** and **9b** as the ratio of MFC/MIC > 4, indicating their promising fungistatic potential (Table 2).

2.2.3. Antituberculosis Efficiency. Furthermore, the new thiophenyl-pyrazolyl-thiazole hybrids were subjected to the in vitro evaluation for their antituberculosis effect against *M. tuberculosis* (RCMB 010126) through applying microplate alamar blue assay, where isoniazid is employed as a reference drug (Table 3). The derivatives **4c** and **6b** presented outstanding antituberculosis efficiency equipotent to that obtained by isoniazid (MIC = 0.12 μg/mL). In addition, the derivatives **8b**, **9b** and **10b** displayed an eminent antituberculosis effect (MICs = 1.95, 1.95, and 0.98 μg/mL, respectively), whereas compounds **2b**, **3b**, **8c** and **9a** revealed modest efficiency (MICs = 15.6, 7.81, 7.81, and 15.6 μg/mL, respectively). However, the antituberculosis efficiency was significantly decreased by the other investigated candidates. It

https://doi.org/10.1021/acsomega.3c04736
ACS Omega 2023, 8, 39250−39268

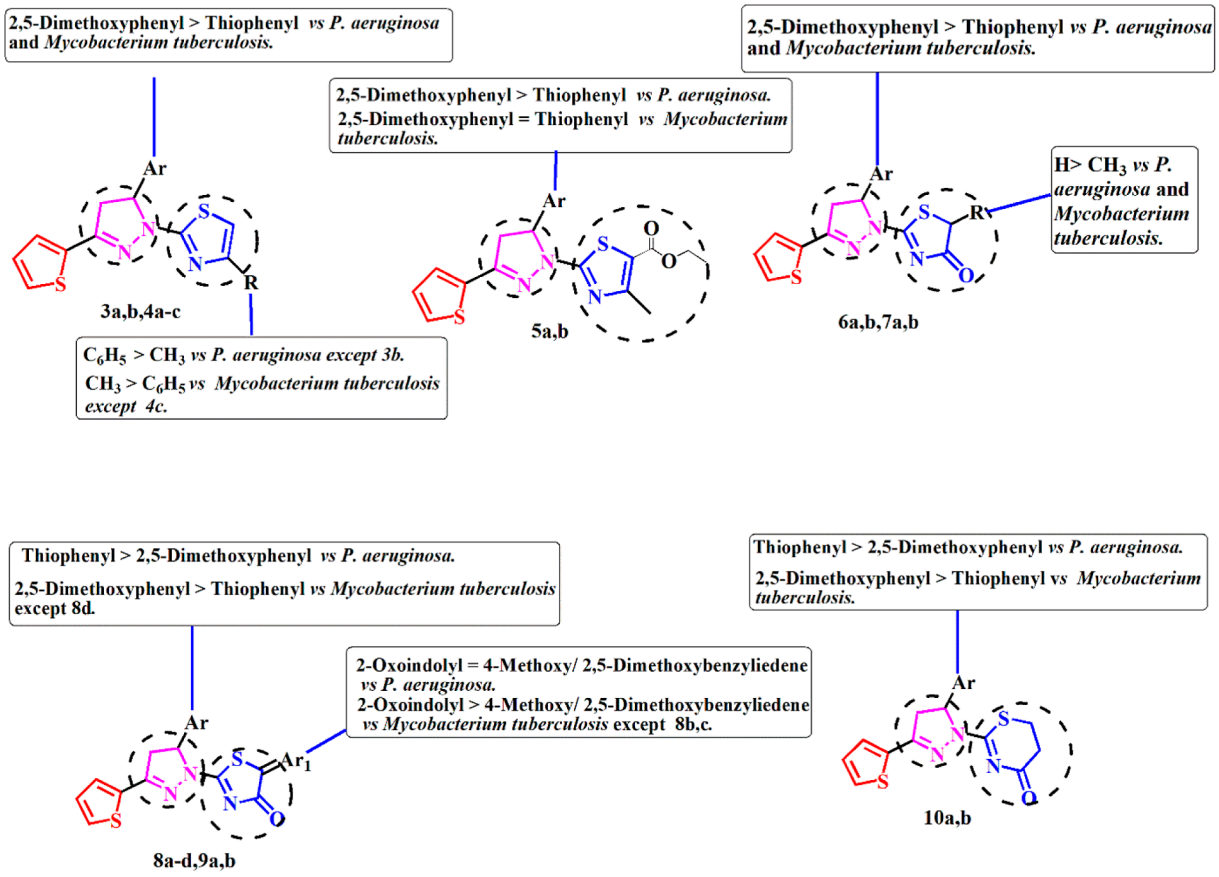

Figure 5. SAR study of the new thiophenyl-pyrazolyl-thiazole hybrids **3**−**10** vs *P. aeruginosa* and *Mycobacterium tuberculosis*.

Table 3. Minimum Inhibitory Concentration (μg/mL) of the New Thiophenyl-pyrazolyl-thiazole Hybrids against Sensitive *Mycobacterium tuberculosis*

compound	MIC (μg/mL)
2b	15.6
3a	62.5
3b	7.81
4a	62.5
4b	31.25
4c	0.12
5a	31.25
5b	31.25
6a	31.25
6b	0.12
7a	62.5
7b	62.5
8a	31.25
8b	1.95
8c	7.81
8d	31.25
9a	15.6
9b	1.95
10a	31.25
10b	0.98
isoniazid	0.12

could be observed that the hybridization of 5-(2,5-dimethoxyphenyl)-3-(thiophen-2-yl) pyrazolyl scaffold with 4-methyl thiazole **3b** resulted in a promising antituberculosis efficiency (MIC = 7.81 μg/mL); however, the activity remarkably declined by approximately 4-fold upon the replacement of methyl with a bulky phenyl substituent as compound **4b** (MIC = 31.25 μg/mL), and also via the substitution of thiazole with an ethyl carboxylate functional group as compound **5b** (MIC = 31.25 μg/mL).

On the other hand, the hybridization of 5-(2,5-dimethoxyphenyl)-3-(thiophen-2-yl) pyrazolyl scaffold with unsubstituted thiazolidinone as compound **6b** afforded a prominent antituberculosis efficacy (MIC = 0.12 μg/mL) equipotent to isoniazid impact. However, the introduction of the 5-methyl group as compound **7b** led to a total loss of the antituberculosis efficiency. Conversely, the replacement of the methyl group with the 4-methoxybenzylidene group **8b** remarkably enhanced the antituberculosis effect (MIC = 1.95 μg/mL); however, the dimethoxy analog **8d** produced weak antituberculosis potency (MIC = 31.25 μg/mL). Moreover, replacing the 4-methoxybenzylidene group with indolinone scaffold as compound **9b** resulted in retaining the remarkable antituberculosis efficacy (MIC = 1.95 μg/mL). In addition, it was observed that the conjugation of 5-(2,5-dimethoxyphenyl)-3-(thiophen-2-yl) pyrazolyl scaffold with thiazinone ring **10b** has a prominent effect in increasing the antituberculosis efficiency (MIC = 0.98 μg/mL). On the other hand, the antituberculosis effect was lost by the 3,5-di(thiophen-2-yl)pyrazolyl analogs except **4c**, **8c,** and **9a** (Figure 5).

2.2.4. DHFR Inhibitory Efficiency. The most efficient antituberculosis agents **4c**, **6b**, **8b**, **9b,** and **10b** have been elected to investigate their inhibitory potency versus *M. tuberculosis* DHFR enzyme. The results compared with trimethoprim are depicted as IC_{50} values in μM in Table 4.

https://doi.org/10.1021/acsomega.3c04736
ACS Omega 2023, 8, 39250−39268

Table 4. Inhibitory Efficiency of Some Potent Thiophenyl-pyrazolyl-thiazole Hybrids against *Mtb* DHFR Enzyme

compound	IC_{50} (μM)
4c	4.21 ± 0.13
6b	5.70 ± 0.28
8b	18.45 ± 0.61
9b	22.73 ± 0.55
10b	10.59 ± 0.31
trimethoprim	6.23 ± 0.05

The thiophenyl-pyrazolyl-thiazole derivatives **4c** and **6b** exhibited a promising inhibitory efficiency against *Mtb* DHFR enzyme with IC_{50} values 4.21 and 5.70 μM, respectively, exceeding that of trimethoprim (IC_{50} = 6.23 μM). Furthermore, compound **10b** displayed significant inhibitory efficiency (IC_{50} = 10.59 μM) relative to trimethoprim. However, the inhibitory potency was declined by compounds **8b** and **9b** (IC_{50} = 18.45 and 22.73 μM, respectively).

2.3. Biodistribution Study. Biodistribution studies are considered a powerful step for investigating the new synthetic compounds.[41] The most applicable technique for the biodistribution analysis is to radiolabel these compounds with an appropriate radionuclide. At different time intervals, the radioactivity uptake of tissues and/or organs is calculated.[42] The radiolabeling of these carriers must be applied and executed under suitable conditions which cause comparatively low or negligible changes in the carrier's structure.[43]

A biodistribution study was rendered for one of the hopeful antimicrobial candidates **6b** as a representative example to explore its in vivo pharmacokinetic behavior and body organ uptakes, besides its elimination pathway via radiolabeling with ^{131}I.[44,45]

2.3.1. Radiolabeling of the Compound ***6b****.* ^{131}I-compound **6b** was simply and rapidly obtained using the oxidizing agent Chloramine-T (CAT) by electrophilic substitution. It is substantial to focus that Chloramine-T is a water-soluble reagent with strong oxidizing properties requiring a briefer reaction time, simplifying the process in nuclear medicine.[46] So, we prepared ^{131}I-**6b** compound with maximum radiochemical efficiency (RE) (95.1 ± 1.53%) that was accomplished using 150 μg of compound **6b** and 150 μg Chloramine-T at pH 7 and 25 °C for 30 min reaction time. The radiolabeling factors were studied in a range of compound **6b** amount (50−250 μg), reaction temperature (25−100 °C), Chloramine-T amount (50−250 μg), reaction time (15−120 min), and pH (2−11) (Figure 6). One-way ANOVA was used as statistical test to evaluate data differences (level of significance set at $P < 0.05$). The radiolabeled compound **6b** showed good in vitro stability up to 24 h.

2.3.2. Biodistribution Study of ^{131}I*-Compound* ***6b*** *in Healthy and Infected Induced Mice.* The in vivo distribution of ^{131}I-compound **6b** was investigated in healthy mice, and the results are presented in (Figure 7a). The resulting ^{131}I-compound **6b** upon using the oxidizing agent Chloramine-T in the existent radiolabeling process showed high renal excretion and rapid blood clearance in all groups (Figure 7a). In healthy mice, the activity eliminated by urine reached 20.2% ± 1.2 represented as % injected dose/gram organ (% ID/g) at 4 h post injection so we concluded that the main excretion pathway of the ^{131}I-compound **6b** is through the renal route. It is considerable to indicate that the very low radioactivity in the thyroid glands proved the in vivo stability of ^{131}I-compound **6b**.

Additionally, we studied the infection targeting ability of ^{131}I-compound **6b** in vivo in the infected Albino mice model, as illustrated in Figure 7b. Target/non-target ratios (T/NT) are the key factors to evaluate the targeting of ^{131}I-compound **6b** to the infection. T/NT ratios are presented in Table 5. The results showed specific and high localization in the infection-site, represented by the right thigh muscle, when compared with the normal tissue, represented by left thigh muscle of the same animal, with a T/NT ratio of 7.8 ± 1.1 within 1 h of introduction into circulation, maintaining values higher than 4 for up to 2 h. Furthermore, it did not exhibit any high accumulation in other body organs.

2.4. Molecular Docking Study. In order to elucidate the difference between the in vitro inhibitory potencies of the screened thiophenyl-pyrazolyl-thiazole hybrids **4c**, **6b**, **8b**, **9b**, and **10b** against *M. tuberculosis* dihydrofolate reductase enzyme, the docking simulation was employed via the software of Molecular Operating Environment (MOE-Dock) version 2014.0901.[47,48] The original cocrystallized ligand trimethoprim was first redocked within the active binding site of *M. tuberculosis* DHFR enzyme (PDB code: 1DG5)[49] to confirm the docking process. The obtained energy score of −10.62 kcal/mol at the root-mean-square deviation (rmsd) value equal to 0.79 Å indicates that the docking process was certified. As shown in Figure 8A, the two amino groups at positions 2 and 4 of pyrimidine moiety formed three H-bonds with the backbones of **Ile5** and **Ile94** and the side chain of **Asp27** (distance: 2.76, 2.85, and 2.81 Å, respectively). Also, the C2 of trimethoxybenzyl displayed arene−H interaction with the centroid of **Phe31**.

After that, our thiophenyl-pyrazolyl-thiazole hybrids **4c**, **6b**, **8b**, **9b**, and **10b** were docked, and the obtained results are illustrated in Figures 8 and 9.

As demonstrated in the 2D view (Figure 8) and 3D (Figure S1), the highly promising inhibitory thiophenyl-pyrazolyl-thiazole hybrids **4c**, **6b**, and **10b** were enclosed within the active pocket of *M. tuberculosis* DHFR with favorable energy scores of −11.26, −11.08, and −10.13 kcal/mol, respectively. It was well-known that the sulfur atom of thiazole moiety in **4c** and **6b** and thiazinone in **10b** afforded H-bond donors with the backbone of the key amino acid **Ile94** (distance: 4.09, 3.60, and 3.42 Å, respectively). Moreover, the existence of thiophene ring at p-5 of pyrazoline scaffold potentiates the inhibitory potency of **4c** through formation of arene−H interaction with **Ile14**.

On the other hand, the lower inhibitory potency of the **8b** and **9b** was illustrated by inspection of the 2D view (Figure 9) and 3D (Figure S2), which displayed the binding within the active pocket of *M. tuberculosis* DHFR with adequate energy scores of −9.22 and −9.17 kcal/mol, respectively. The presence of 4-methoxybenzylidene in **8b** and 2-oxoindolin-3-ylidene in **9b** at p-5 of thiazole scaffold pushed the thiazolone moiety away from binding with **Ile94** and facilitated the chance for binding with **Phe31** through arene−arene interactions. Furthermore, the 4-methoxybenzylidene in **8b** exhibited arene−H interaction with **Trp6**, while the nitrogen of 2-oxoindolin-3-ylidene in **9b** revealed the H-bond donor with the backbone of **Ala7** (distance: 3.58 Å).

As concluded from the previous data, the existence of the pyrazoline core substituted at p-1 with thiazole bearing 4-

https://doi.org/10.1021/acsomega.3c04736
ACS Omega 2023, 8, 39250−39268

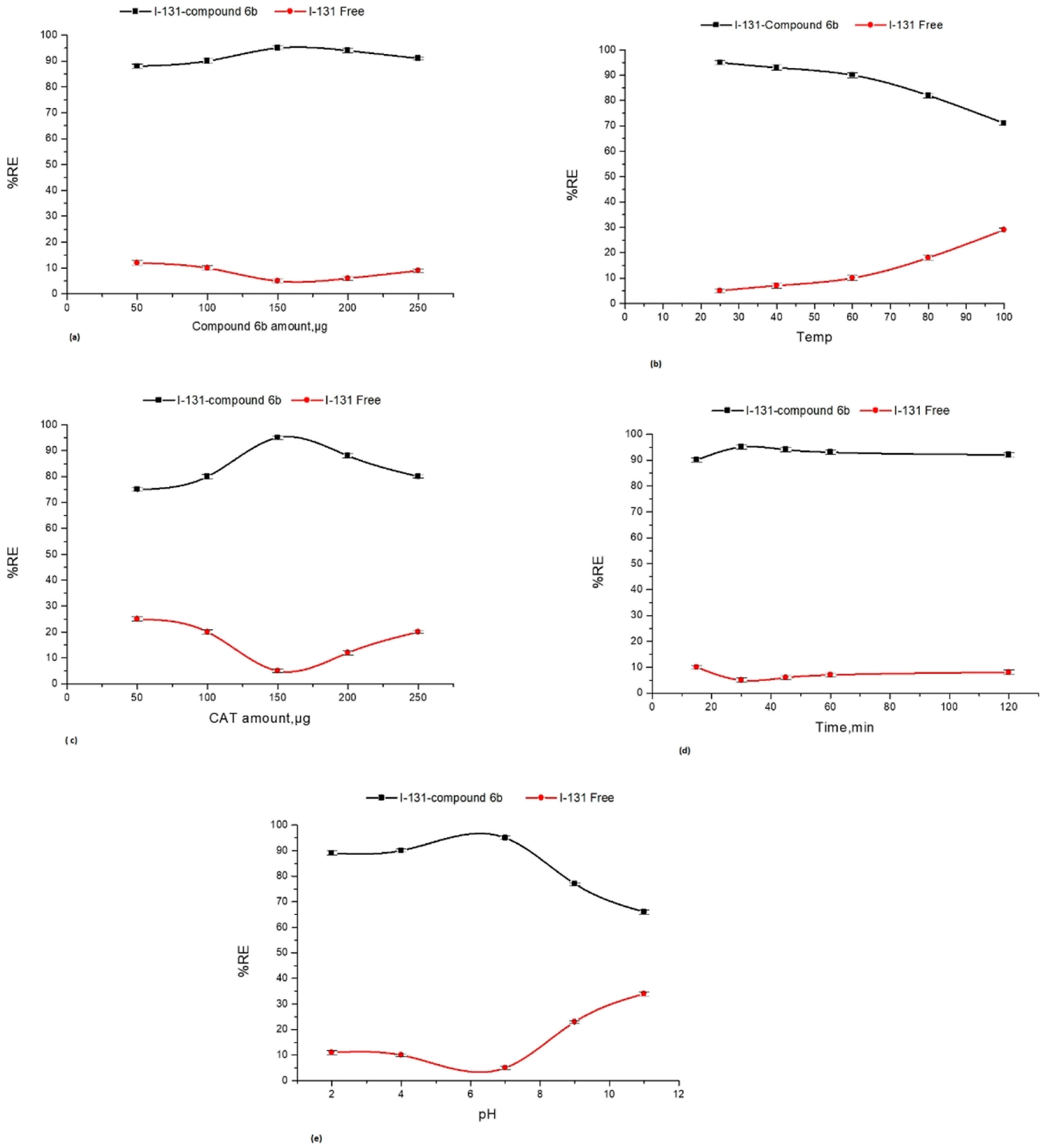

Figure 6. Variation of % RE of ^{131}I-compound **6b** as a function of (a) compound **6b** amount, μg; (b) temp (c) Chloramine-T amount, μg; (d) reaction time, min; (e) pH.

bromophenyl (i.e., electron-withdrawing group) in **4c**, unsubstituted thiazolone in **6b,** or thiazinone in **10b** promoted favorable hydrogen bonding with the key amino acid **Ile94** and gave the chance for more fitting within the active pocket of *M. tuberculosis* DHFR. Conversely, substitution of the thiazolone ring at p-5 with 4-methoxybenzylidene in **8b** and 2-oxoindolin-3-ylidene in **9b** devoted them from the valuable binding with **Ile94** and that could be the reason for their lower inhibitory potencies with *M. tuberculosis* DHFR.

2.5. In Silico ADMET Prediction Study. Examination of absorption, distribution, metabolism, and excretion (ADME) for the targeted substances can provide significant details about the best drug choice. This anticipated study was facilitated by the use of SwissADME, a free online tool.[50,51]

The Veber rule (TPSA $\leq$ 140 Å^2, number of rotatable bonds $\leq$10) and Lipinski's rule (MW $\leq$ 500, number of H-bond donors $\leq$5, number of hydrogen bond acceptors $\leq$10 and MLog P $\leq$ 4.15) govern the optimal medication for oral

https://doi.org/10.1021/acsomega.3c04736
ACS Omega 2023, 8, 39250−39268

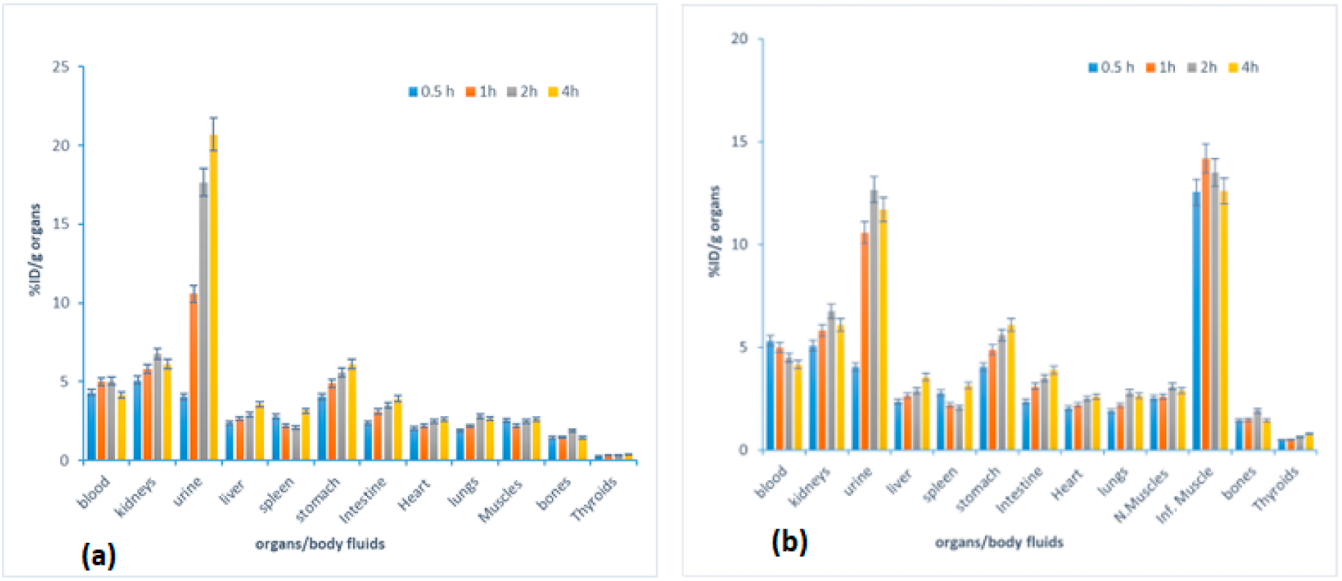

Figure 7. In vivo biodistribution of ^{131}I-compound **6b** in healthy mice (a) and infection-induced models (b) following I.V. injection at different time intervals.

Table 5. Infection Targeting Ability of ^{131}I-Compound 6b Following I.V. Injection at Different Time Intervals

time p.i.,h	T/NT uptake ratio
0.5	6.5 ± 1.1
1	7.8 ± 1.1
2	4.5 ± 1.2
4	3.4 ± 0.8

administration (Table 6). With the exception of **4c**, which demonstrated MLog P > 4.15 and one violation, the screened thiophenylpyrazolyl-thiazole hybrids **6b** and **10b** were identified to be in accordance with the previous rules.

According to the bioavailability radar chart, the screened thiophenyl-pyrazolyl-thiazole hybrids **6b** and **10b** are located in the ideal range (pink area) in relation to all six key variables (lipophilicity, size, polarity, solubility, saturation, and flexibility), which supplied a good expectation for their oral bioavailability (Figure 10). The derivative **4c**, on the other hand, stayed far from the ideal regions of lipophilicity, solubility, saturation, and flexibility, and it was anticipated that it would not be orally bioavailable.

Table S1 in Supporting Information and Figure 11 provide an analysis of the pharmacokinetic properties concerning the potential thiophenyl-pyrazolyl-thiazole hybrids **4c**, **6b**, and **10b**. The Boiled-Egg chart's white region and away from the yellow one is where the thiophenyl-pyrazolyl-thiazole hybrids **6b** and **10b** were found, suggesting that there was no BBB penetration along with an elevated probability of gastrointestinal absorption. The derivative **4c**, on the other hand, was far from both regions, resulting in weak predicted gut absorption. As a result, they are restricted to treating peripheral infections and are not anticipated to have any negative impacts on the central nervous system. These targets also had a high bioavailability value of 0.55 and are not predicted to set off a PAIN alarm.

The drug efflux transporter P-glycoprotein (P-gp), which is known to move drugs out of cells, may be one of the reasons of drug tolerance. The screened derivatives **6b** and **10b** are P-gp nonsubstrates, as forecasted from the SwissADME Web site (red dots in Figure 11), suggesting little chance of their efflux out of the cell with a maximal activity other than compound **4c** (blue dot, P-gp substrate).

The expected toxicity characteristics of the potent thiophenyl-pyrazolyl-thiazole hybrids **4c**, **6b,** and **10b** set in Table 7 displayed no inhibition of human ether-a-go-go-related gene (hERG) potassium channel, indicating no danger of cardiotoxicity and no cardiac adverse effects that constitute significant issues in clinical investigations of drug applicants. Additionally, all screened targets achieved no Ames toxicity, which should be assessed in the early phases of drug discovery to gauge the possibility of genotoxicity for the investigated molecule. According to calculations of the acute oral toxicity, the thiophenyl-pyrazolyl-thiazole hybrids **4c**, **6b,** and **10b** afforded the values of 567.2, 517.8, and 582.2 mg kg^{-1}, respectively, that fall in the third category (500 mg kg^{-1} < LD50 ≤ 5000 mg kg^{-1}) and hence create them nontoxic molecules. Furthermore, the carcinogenicity descriptor (CARC) values of 526.1, 569, and 530 mg kg^{-1} body weight per day suggested that these molecules could be classified as noncarcinogenic and nonrequired. Concerning biodegradation assessment in the environment, it was supposed that all derivatives could be identified for not-ready biodegradable chemicals.

3. CONCLUSIONS

New thiophenyl-pyrazolyl-thiazole hybrids **3**−**10** were designed, synthesized, and screened for their antibacterial efficiency against Gram − and Gram + bacterial strains. It was clearly apparent that new thiophenyl-pyrazolyl-thiazole hybrids demonstrated remarkable antibacterial efficacy versus Gram − bacteria more than Gram + bacteria compared to the reference drug amoxicillin. The antibacterial evaluation displayed the significant sensitivity of the Gram − bacteria *P. aeruginosa* toward all of the screened candidates except for compounds (**3a**, **5a,** and **7a**) with MICs values ranging from 3.9 to 125 μg/mL comparing to amoxicillin with MIC > 500 μg/mL. Also, most of the investigated analogs exhibited

https://doi.org/10.1021/acsomega.3c04736
ACS Omega 2023, 8, 39250−39268

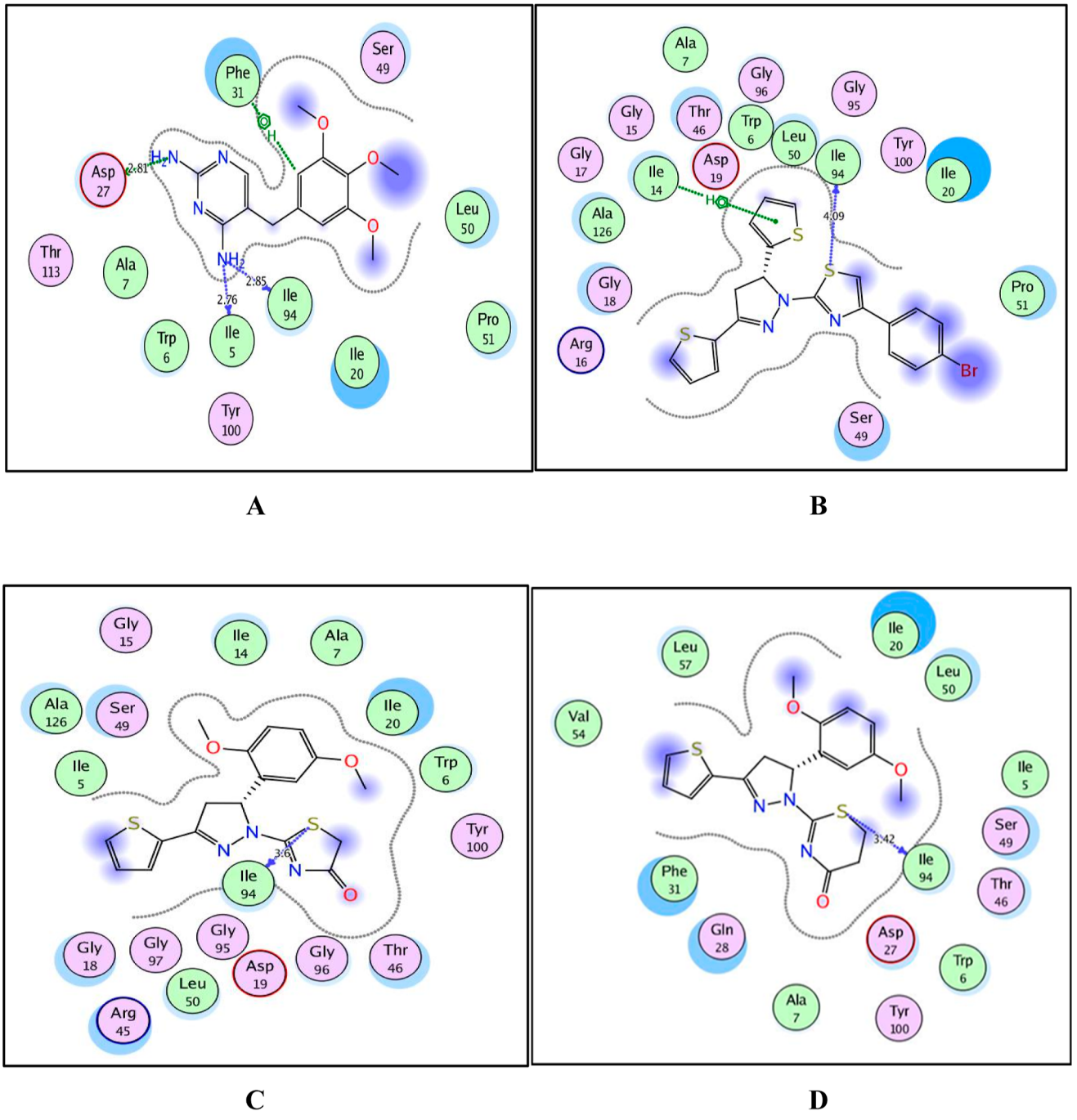

Figure 8. A, B, C, and D patterns clarifying the 2D binding poses of trimethoprim and the promising thiophenyl-pyrazolyl-thiazole hybrids **4c**, **6b**, and **10b** into the active pocket of *M. tuberculosis* DHFR, respectively (PDB code: 1DG5).

reasonable antibacterial efficacy against *E. coli* with MICs of 62.5−125 μg/mL relative to amoxicillin (MIC = 62.5 μg/mL).

However, the examined hybrids appeared to be inactive as antibacterial candidates versus Gram + bacterial strain *S. aureus*. While compounds **4a** and **5a** presented prominent antibacterial efficiency against *B. subtilis* with MICs = 15.625 and 3.9 μg/mL, respectively, compared to amoxicillin (MIC = 31.25 μg/mL). In addition, all the examined analogs revealed noticeable antifungal efficacy with MICs (3.9−125 μg/mL) relative to fluconazole (MIC = 250 μg/mL). Moreover, compounds **4c**, **6b**, **8b**, **9b**, and **10b** displayed remarkable antituberculosis efficiency (MICs = 0.12−1.95 μg/mL) compared with the reference drug isoniazid (MIC = 0.12 μg/mL). The former derivatives were assessed for their suppression potency versus *M. tuberculosis* DHFR enzyme, compounds **4c**, **6b**, and **10b** demonstrated outstanding suppression effect with IC_{50} values of 4.21, 5.70, and 10.59 μM, respectively, compared to that of trimethoprim (IC_{50} = 6.23 μM).

The pharmacokinetic pattern of compound **6b** (selected as a representative example) was studied by radiosynthesis of the ^{131}I- compound **6b** and optimized with a radiochemical efficiency of 95.1% at pH 7, 150 μg Chloramine-T amount, 150 μg compound **6b** amount, and 30 min reaction time. The biodistribution pattern showed a notable accumulation of radioactivity in infected muscle compared to normal muscle

https://doi.org/10.1021/acsomega.3c04736
ACS Omega 2023, 8, 39250−39268

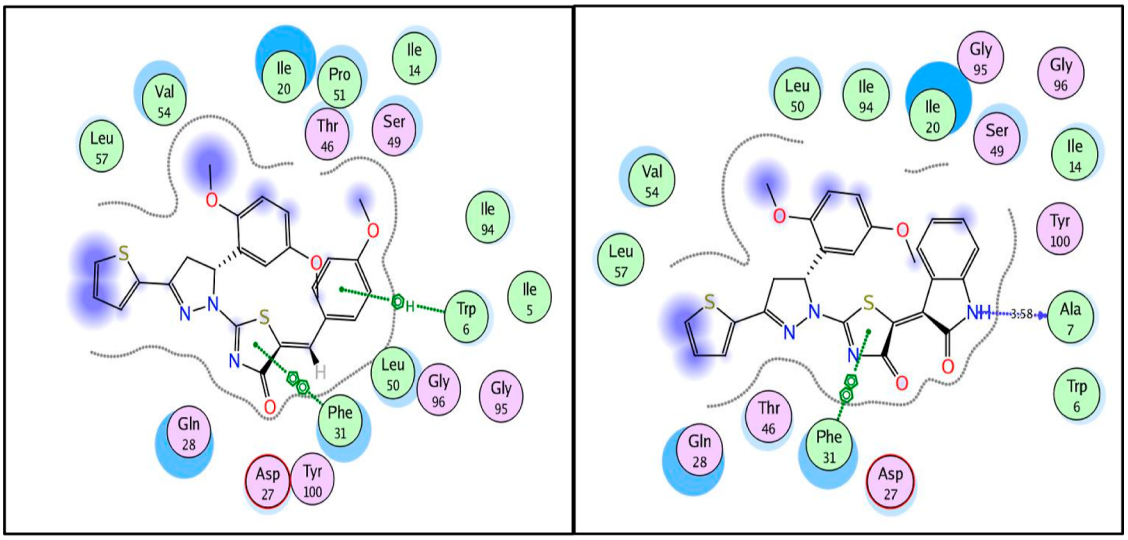

Figure 9. A and B patterns clarifying the 2D binding poses of the lower inhibitory potency thiophenyl-pyrazolyl-thiazole hybrids **8b** and **9b** into the active pocket of *M. tuberculosis* DHFR, respectively (PDB code: 1DG5).

Table 6. Anticipated Physicochemical Features of the Potent Thiophenyl-pyrazolyl-thiazole Hybrids 4c, 6b and 10b

compd.	MW[a]	TPSA (Å^2)[b]	nRB[c]	nHBA[d]	nHBD[e]	MLog P[f]	violations[g]
4c	472.44	113.21	4	2	0	4.26	1
6b	387.48	117.03	5	5	0	2.00	0
10b	401.50	117.03	5	5	0	2.24	0

[a]Molecular weight. [b]Calculated lipophilicity (MLog $P_{o/w}$). [c]Number of the rotatable bond. [d]Number of the hydrogen bond acceptor. [e]Number of the hydrogen bond donor. [f]Topological polar surface area. [g]Violations from Lipinski and Veber rules.

(high T/NT) of the infected mice. The docking study for the new hybrids **4c**, **6b**, **8b**, **9b,** and **10b** was carried out to identify the various binding interactions with *Mtb* DHFR enzyme and reflected their well-fitting within the active pocket with promising energy scores ranging from −9.17 to −11.26 kcal/mol in comparison with native ligand trimethoprim (−10.62 kcal/mol). In silico ADMET studies revealed that the potent inhibitors **4c**, **6b,** and **10b** attained the criterion of the drug likeness approach.

4. EXPERIMENTAL SECTION

4.1. Chemistry. All melting points are uncorrected and were taken in open capillary tubes using Electrothermal apparatus 9100. Elemental microanalyses were carried out at Microanalytical Unit, Central Services Laboratory, National Research Centre, Dokki, Cairo, Egypt, using Vario Elementar. Infrared spectra were recorded on a Schimadzu FT-IR Affinity-1 Spectrometer, Infrared spectrometer at cm^{-1} scale using KBr disc technique. ^{1}H NMR and ^{13}C NMR spectra were determined by using a Bruker High Performance Digital FT-NMR Spectrometer Avance III 400 MHz. Chemical shifts were expressed in δ (ppm) downfield from TMS as an internal standard. The mass spectra were measured with a Finnigan MATSSQ-7000 mass spectrometer. The reactions were pursued by TLC (aluminum sheets, Merck), and the spots were disclosed by exposure to UV lamp. Compound **2a**[52] were prepared as previously described in Literature.

*4.1.1. General Procedure for the Synthesis of Derivatives **2a,b**.* A mixture of the appropriate chalcones **1a,b** (0.01 mol) and thiosemicarbazide (0.01 mol, 0.91gm) and potassium hydroxide (1.12 g, 0.02 mol) in absolute ethanol (20 mL) was heated under reflux for 8 h. The reaction mixture was cooled and poured onto ice/water. The formed precipitate was filtered, dried, and recrystallized from ethanol to afford the corresponding compound **2a,b**, respectively.

*4.1.1.1. 4,5-Dihydro-5-(2,5-dimethoxyphenyl)-3-(thiophen-2-yl)pyrazole-1-carbothioamide (**2b**).* Colorless crystals; mp: 270−272 °C; yield: 80%. IR (cm^{-1}): 3388, 3219 (NH_2), 1225 (C═S), 1598 (C═N). ^{1}H NMR (DMSO-d_6): δ 2.96 (dd, J = 17.6, 2.8 Hz, 1H, pyrazoline-H_4), 3.64 (s, 3H, OCH_3), 3.79 (s, 3H, OCH_3), 3.85 (dd, J = 17.6, 11.2 Hz, 1H, pyrazoline-H_4'), 6.02 (dd, J = 10.8, 2.8 Hz, 1H, pyrazoline-H_5), 6.34 (d, J = 2.4 Hz, 1H, Ar−H), 6.79 (d, J = 8.8 Hz, 1H, Ar−H), 6.95 (s, 1H, Ar−H), 7.12 (d, J = 8.4 Hz, 1H, Ar−H), 7.47(d, J = 3.6 Hz, 1H, Ar−H), 7.61 (s, 1H, NH, exchangeable with D_2O), 7.76 (d, J = 5.2 Hz, 1H, Ar−H), 8.03 (s, 1H, NH, exchangeable with D_2O). MS: m/z (%) 347 (M^+, 46.17). Anal. Calcd for $C_{16}H_{17}N_3O_2S_2$ (347.46): C, 55.31; H, 4.93; N, 12.09. Found: C, 55.48; H, 4.80; N, 12.23.

*4.1.2. General Procedure for the Synthesis of Derivatives **3a,b**, **4a−c,** and **5a,b**.* A mixture of the pyrazole-1-carbothioamides **2a,b** (0.01 mol) and the appropriate α-haloketones, chloroacetone, phenacyl bromide, 4-bromo phenacyl bromide, and/or ethyl-2-chloroacetoacetate (0.01 mol) in absolute ethanol (30 mL) in the presence of anhydrous sodium acetate (1.64 g, 0.02 mol) was refluxed for 6−8 h. The precipitate formed after cooling, was filtered, washed with water, dried, and crystallized from ethanol to give the title compounds **3a,b, 4a−c,** and **5a,b**, respectively.

*4.1.2.1. 4,5-Dihydro-1-(4-methylthiazol-2-yl)-3,5-di-(thiophen-2-yl)-1H-pyrazole (**3a**).* Brown crystals; mp 110−

https://doi.org/10.1021/acsomega.3c04736
ACS Omega 2023, 8, 39250−39268

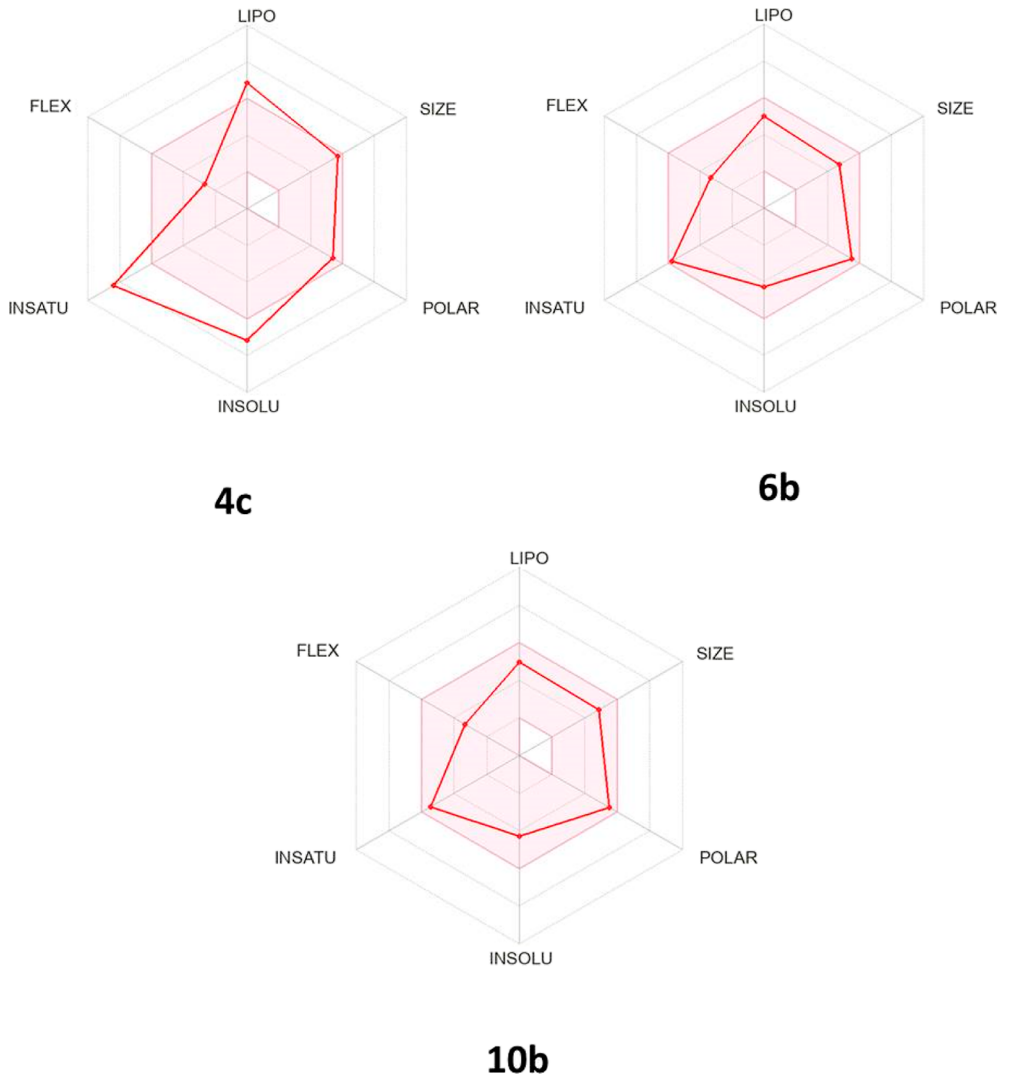

Figure 10. Bioavailability radar chart of the potent thiophenyl-pyrazolyl-thiazole hybrids **4c**, **6b**, and **10b**. The ideal value for each oral bioavailability factor was shown in the pink region, and the expected ones for the assessed molecules were shown as red lines.

112 °C; yield: 73%. IR (cm^{-1}): 1602 (C═N). ^1H NMR (DMSO-d_6): δ 2.13 (s, 3H, CH_3), 3.41 (dd, J = 17.8, 4.2 Hz, 1H, pyrazoline-H_4), 3.96 (dd, J = 17.0, 11.8 Hz, 1H, pyrazoline-H_4'), 5.90 (dd, J = 10.2, 4.2 Hz, 1H, pyrazoline-H_5), 6.48 (s, 1H, thiazole-H_5), 6.98 (br s, 1H, Ar−H), 7.12 (br s, 1H, Ar−H), 7.17 (br s, 1H, Ar−H), 7.41(d, J = 3.6 Hz, 1H, Ar−H), 7.46 (br s, 1H, Ar−H), 7.72 (d, J = 3.6 Hz, 1H, Ar−H). MS: m/z (%) 331 (M^+, 30.91). Anal. Calcd for $C_{15}H_{13}N_3S_3$ (331.48): C, 54.35; H, 3.95; N, 12.68. Found: C, 54.55; H, 4.07; N, 12.52.

*4.1.2.2. 4,5-Dihydro-5-(2,5-dimethoxyphenyl)-1-(4-methylthiazol-2-yl)-3-(thiophen-2-yl)-1H-pyrazole (**3b**).* Brown crystals; mp 119−121 °C; yield: 79%. IR (cm^{-1}): 1608 (C═N). ^1H NMR (DMSO-d_6): δ 2.06 (s, 3H, CH_3), 3.06 (dd, J = 17.6, 5.2 Hz, 1H, pyrazoline-H_4), 3.62 (s, 3H, OCH_3), 3.81(s, 3H, OCH_3), 3.94 (dd, J = 17.4, 11.8 Hz, 1H, pyrazoline-H_4'), 5.68 (dd, J = 11.8, 5.4 Hz, 1H, pyrazoline-H_5), 6.44 (s, 1H, thiazole-H_5), 6.49 (d, J = 3.2 Hz, 1H, Ar−H), 6.81 (d, J = 8.8 Hz, 1H, Ar−H), 6.99 (s, 1H, Ar−H), 7.11 (d, J = 8.8 Hz, 1H, Ar−H), 7.37 (d, J = 2.8 Hz, 1H, Ar−H), 7.68 (d, J = 4.8 Hz, 1H, Ar−H). ^{13}C NMR (DMSO-d_6): δ 17.81, 43.42, 55.72, 56.53, 60.03, 104.22, 112.40, 112.91, 113.19, 128.47, 129.38, 129.90, 130.60, 134.64, 149.06, 149.21, 150.61, 153.45, 164.50. MS: m/z (%) 385 (M^+, 26.11). Anal. Calcd for $C_{19}H_{19}N_3O_2S_2$ (385.5): C, 59.20; H, 4.97; N, 10.90. Found: C, 59.41; H, 4.85; N, 10.99.

*4.1.2.3. 4,5-Dihydro-1-(4-phenylthiazol-2-yl)-3,5-di(thiophen-2-yl)-1H-pyrazole (**4a**).* Brown crystals; mp 148−150 °C; yield: 80%. IR (cm^{-1}): 1610 (C═N). ^1H NMR (DMSO-d_6): δ 3.54 (dd, J = 16.6, 6.6 Hz, 1H, pyrazoline-H_4), 4.03 (dd, J = 17.2, 11.6 Hz, 1H, pyrazoline-H_4'), 6.00 (dd, J = 11.4, 5.4 Hz, 1H, pyrazoline-H_5), 7.01 (t, J = 3.6 Hz, 1H, Ar−H), 7.19 (t, J = 3.8 Hz, 1H, Ar−H), 7.26−7.41(m, 5H, Ar−H and thiazole-H_5), 7.45 (d, J = 4.8 Hz, 1H, Ar−H), 7.51 (d, J = 2.8 Hz, 1H, Ar−H), 7.75 (d, J = 4.8 Hz, 1H, Ar−H), 7.83 (d, J = 7.6 Hz, 2H, Ar−H). ^{13}C NMR (DMSO-d_6): δ 43.97, 60.29, 105.18, 126.05, 126.13, 126.37, 127.22, 128.07, 128.59, 129.02, 129.86, 130.42, 134.32, 134.93, 144.17, 149.55, 150.96, 164.66. MS: m/z (%) 393 (M^+, 55.20). Anal. Calcd for $C_{20}H_{15}N_3S_3$ (393.55): C, 61.04; H, 3.84; N, 10.68. Found: C, 61.22; H, 3.77; N, 10.55.

*4.1.2.4. 4,5-Dihydro-5-(2,5-dimethoxyphenyl)-1-(4-phenylthiazol-2-yl)-3-(thiophen-2-yl)-1H-pyrazole (**4b**).* Brown crystals; mp 170−172 °C; yield: 78%. IR (cm^{-1}): 1612 (C═N). ^1H NMR (DMSO-d_6): δ 3.23 (dd, J = 17.6, 6.0 Hz, 1H, pyrazoline-H_4), 3.66 (s, 3H, OCH_3), 3.79 (s, 3H, OCH_3),

https://doi.org/10.1021/acsomega.3c04736
ACS Omega 2023, 8, 39250−39268

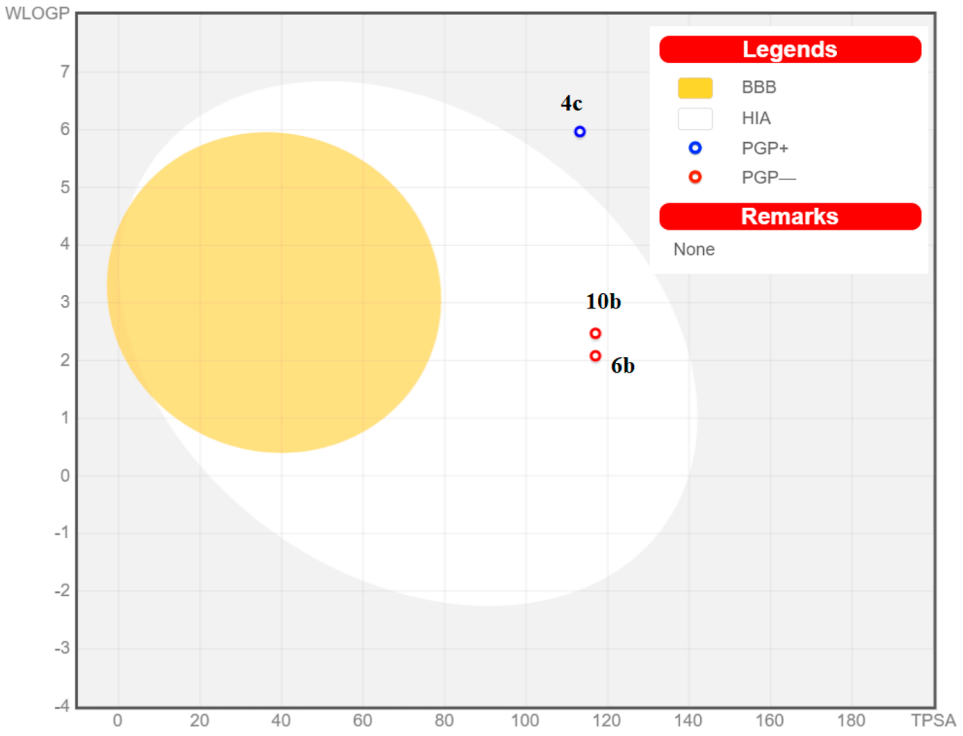

Figure 11. Image of a Boiled-Egg showing the capacity of the potent thiophenyl-pyrazolyl-thiazole hybrids **4c**, **6b**, and **10b** to penetrate the blood–brain barrier and be absorbed by the gastrointestinal tract; PGP+: P-glycoprotein substrate; PGP-: P-glycoprotein nonsubstrate.

Table 7. Anticipated Toxicity Properties of the Thiophenyl-pyrazolyl-thiazole Hybrids 4c, 6b, and 10b

	probability		
toxicity	**4c**	**6b**	**10b**
hERG inhibition T_hERG_I	0.9402 (weak inhibitor)	0.9831 (weak inhibitor)	0.9565 (weak inhibitor)
hERG inhibition T_hERG_II	0.8971 (noninhibitor)	0.8622 (noninhibitor)	0.6759 (noninhibitor)
AMES toxicity	0.5156 (non AMES toxic)	0.5175 (non AMES toxic)	0.5120 (non AMES toxic)
carcinogens	0.8017 (noncarcinogens)	0.8218 (noncarcinogens)	0.8701 (noncarcinogens)
acute oral toxicity (AO)	0.5672 (III)	0.5178 (III)	0.5822(III)
carcinogenicity (three-class)	0.5261 (nonrequired)	0.5690 (nonrequired)	0.5300 (nonrequired)
biodegradation	1.0000 (not-ready biodegradable)	0.6472 (not-ready biodegradable)	0.7923 (not-ready biodegradable)

3.95 (dd, J = 17.2, 12.0 Hz, 1H, pyrazoline-H_4'), 5.79 (dd, J = 12.2, 6.2 Hz, 1H, pyrazoline-H_5), 6.74 (d, J = 3.2 Hz, 1H, Ar–H), 6.82 (d, J = 8.8 Hz, 1H, Ar–H), 6.99 (s, 1H, Ar–H), 7.14 (d, J = 8.4 Hz, 1H, Ar–H), 7.25 (t, J = 7.4 Hz, 1H, Ar–H), 7.31 (s, 1H, thiazole-H_5), 7.34 (t, J = 7.4 Hz, 2H, Ar–H), 7.41 (d, J = 3.6 Hz, 1H, Ar–H), 7.70–7.73 (m, 3H, Ar–H). MS: m/z (%) 447 (M^+, 48.33). Anal. Calcd for $C_{24}H_{21}N_3O_2S_2$ (447.57): C, 64.40; H, 4.73; N, 9.39. Found: C, 64.29; H, 4.79; N, 9.51.

*4.1.2.5. 1-(4-(4-Bromophenyl)thiazol-2-yl)-4,5-dihydro-3,5-di(thiophen-2-yl)-1H-pyrazole (**4c**).* Brown crystals; mp 188–190 °C; yield: 87%. IR (cm^{-1}): 1602 (C═N). ^{1}H NMR (DMSO-d_6): δ 3.58 (dd, J = 15.4, 7.8 Hz, 1H, pyrazoline-H_4), 4.03 (dd, J = 17.6, 11.2 Hz, 1H, pyrazoline-H_4'), 6.00 (dd, J = 11.2, 5.6 Hz, 1H, pyrazoline-H_5), 6.98 (d, J = 3.6 Hz, 1H, Ar–H), 7.18 (d, J = 3.6 Hz, 1H, Ar–H), 7.24 (d, J = 3.2 Hz, 1H, Ar–H), 7.44 (s, 1H, thiazole-H_5), 7.52 (d, J = 4.4 Hz, 1H, Ar–H), 7.58 (d, J = 8.4 Hz, 2H, Ar–H), 7.75–7.79 (m, 2H, Ar–H), 7.85 (d, J = 8.4 Hz, 1H, Ar–H), 7.99 (d, J = 8.4 Hz, 1H, Ar–H). MS: m/z (%) 472 (M^+, 100). Anal. Calcd for $C_{20}H_{14}BrN_3S_3$ (472.44): C, 50.84; H, 2.99; N, 8.89. Found: C, 50.77; H, 3.07; N, 8.95.

*4.1.2.6. Ethyl 2-(4,5-dihydro-3,5-di(thiophen-2-yl)pyrazol-1-yl)-4-methylthiazole-5-carboxylate (**5a**).* Yellow crystals; mp 124–126 °C; yield: 84%. IR (cm^{-1}): 1727 (C═O), 1605 (C═N). ^{1}H NMR (DMSO-d_6): δ 1.26 (t, J = 6.8 Hz, 3H, CH_3), 2.43 (s, 3H, CH_3), 3.53 (dd, J = 17.4, 3.0 Hz, 1H, pyrazoline-H_4), 4.01 (dd, J = 17.8, 11.4 Hz, 1H, pyrazoline-H_4'), 4.19 (q, J = 6.6 Hz, 2H, CH_2), 6.03 (dd, J = 11.0, 3.0 Hz, 1H, pyrazoline-H_5), 6.98 (d, J = 3.6 Hz, 1H, Ar–H), 7.13 (br s, 1H, Ar–H), 7.20 (br s, 1H, Ar–H), 7.44 (d, J = 4.4 Hz, 1H, Ar–H), 7.57 (d, J = 3.6 Hz, 1H, Ar–H), 7.80 (d, J = 4.4 Hz, 1H, Ar–H). ^{13}C NMR (DMSO-d_6): δ 14.72, 17.91, 44.29, 59.48, 60.69, 111.20, 126.15, 127.37, 128.72, 130.79, 131.44, 133.75, 143.58, 151.79, 159.49, 162.23, 164.97. MS: m/z (%) 403 (M^+, 23.81). Anal. Calcd for $C_{18}H_{17}N_3O_2S_3$ (403.54): C, 53.57; H, 4.25; N, 10.41. Found: C, 53.48; H, 4.33; N, 10.50.

*4.1.2.7. Ethyl 2-(4,5-dihydro-5-(2,5-dimethoxyphenyl)-3-(thiophen-2-yl)pyrazol-1-yl)-4-methylthiazole-5-carboxylate (**5b**).* Brown crystals; mp 95–97 °C; yield: 87%. IR (cm^{-1}): 1728 (C═O), 1610 (C═N). ^{1}H NMR (DMSO-d_6): δ 1.26 (t, J = 7.0 Hz, 3H, CH_3), 2.36 (s, 3H, CH_3), 3.17 (dd, J = 17.6, 4.4 Hz, 1H, pyrazoline-H_4), 3.63 (s, 3H, OCH_3), 3.79 (s, 3H, OCH_3), 3.98 (dd, J = 17.6, 11.6 Hz, 1H, pyrazoline-H_4'),4.17 (q, J = 6.9 Hz, 2H, CH_2), 5.77 (dd, J = 11.8, 4.6 Hz, 1H,

https://doi.org/10.1021/acsomega.3c04736
ACS Omega 2023, 8, 39250–39268

pyrazoline-H_5), 6.47 (d, J = 2.8 Hz, 1H, Ar−H), 6.83 (d, J = 8.8 Hz, 1H, Ar−H), 6.99 (s, 1H, Ar−H), 7.14 (d, J = 8.8 Hz, 1H, Ar−H), 7.47 (d, J = 3.6 Hz, 1H, Ar−H), 7.77(d, J = 4.8 Hz, 1H, Ar−H). ^{13}C NMR (DMSO-d_6): δ 14.73, 17.90, 43.59, 55.77, 56.58, 59.75, 60.63, 110.71, 112.83, 113.13, 113.26, 128.64, 129.73, 130.50, 131.10, 133.97, 150.62, 152.14, 153.47, 159.71, 162.27, 164.87. MS: m/z (%) 457 (M^+, 66.38). Anal. Calcd for $C_{22}H_{23}N_3O_4S_2$ (457.57): C, 57.75; H, 5.07; N, 9.18. Found: C, 57.66; H, 5.18; N, 9.10.

4.1.3. General Procedure for the Synthesis of Derivatives ***6a,b***. A mixture of the pyrazole-1-carbothioamides **2a,b** (0.01 mol) and ethyl bromoacetate (1.67 mL, 0.01 mol) was dissolved in absolute ethanol (30 mL) containing a few drops of piperidine and the reaction mixture was refluxed for 3 h. The formed precipitate was filtered, dried, and crystallized from ethanol to give the title compounds **6a,b**, respectively.

*4.1.3.1. 2-(4,5-Dihydro-3,5-di(thiophen-2-yl)pyrazol-1-yl)-thiazol-4(5H)-one (**6a**).* Brown crystals; mp 170−172 °C; yield: 75%. IR (cm^{-1}): 1675 (C═O), 1602 (C═N). ^{1}H NMR (DMSO-d_6): δ 3.60 (dd, J = 18.0, 3.6 Hz, 1H, pyrazoline-H_4), 3.96 (s, 2H, CH_2), 4.07 (dd, J = 18.0, 10.8 Hz, 1H, pyrazoline-H_4'), 6.10 (dd, J = 10.8, 3.2 Hz, 1H, pyrazoline-H_5), 7.00 (t, J = 4.2 Hz, 1H, Ar−H), 7.12 (d, J = 3.6 Hz, 1H, Ar−H), 7.24 (t, J = 4.2 Hz, 1H, Ar−H), 7.48 (d, J = 4.8 Hz, 1H, Ar−H), 7.69 (d, J = 3.6 Hz, 1H, Ar−H), 7.89 (d, J = 4.8 Hz, 1H, Ar−H). MS: m/z (%) 333 (M^+, 100). Anal. Calcd for $C_{14}H_{11}N_3OS_3$ (333.45): C, 50.43; H, 3.33; N, 12.60. Found: C, 50.55; H, 3.20; N, 12.70.

*4.1.3.2. 2-(4,5-Dihydro-5-(2,5-dimethoxyphenyl)-3-(thiophen-2-yl)pyrazol-1-yl)thiazol-4(5H)-one (**6b**).* Buff crystals; mp 168−170 °C; yield: 79%. IR (cm^{-1}): 1679 (C═O), 1605 (C═N). ^{1}H NMR (DMSO-d_6): δ 3.25 (dd, J = 18.0, 4.0 Hz, 1H, pyrazoline-H_4), 3.66 (s, 3H, OCH_3), 3.76 (s, 3H, OCH_3), 3.95 (s, 2H, CH_2), 4.03 (dd, J = 17.8, 11.4 Hz, 1H, pyrazoline-H_4'), 5.80 (dd, J = 11.2, 4.0 Hz, 1H, pyrazoline-H_5), 6.45 (d, J = 2.8 Hz, 1H, Ar−H), 6.87 (d, J = 8.8 Hz, 1H, Ar−H), 7.00 (s, 1H, Ar−H), 7.19 (d, J = 8.8 Hz, 1H, Ar−H), 7.59 (d, J = 3.6 Hz, 1H, Ar−H), 7.85 (d, J = 5.2 Hz, 1H, Ar−H). MS: m/z (%) 387 (M^+, 42.50). Anal. Calcd for $C_{18}H_{17}N_3O_3S_2$ (387.48): C, 55.80; H, 4.42; N, 10.84. Found: C, 55.90; H, 4.34; N, 10.60.

4.1.4. General Procedure for the Synthesis of Derivatives ***7a,b***. A mixture of the pyrazole-1-carbothioamides **2a,b** (0.01 mol), ethyl-2-bromopropionate (1.81 mL, 0.01 mol) and catalytic sodium acetate anhydrous (1.64 g, 0.02 mol) in absolute ethanol (20 mL) was refluxed for 8−10 h. After cooling, the precipitate was filtered, washed with water, dried, and recrystallized from ethanol to give the target compounds **7a,b**.

*4.1.4.1. 2-(4,5-Dihydro-3,5-di(thiophen-2-yl)pyrazol-1-yl)-5-methylthiazol-4(5H)-one (**7a**).* Yellow crystals; mp 158−160 °C; yield: 84%. IR (cm^{-1}): 1720 (C═O), 1595 (C═N). ^{1}H NMR (DMSO-d_6): δ 1.48 (d, J = 7.6 Hz, 3H, CH_3), 3.61 (dd, J = 18.0, 3.6 Hz, 1H, pyrazoline-H_4), 4.06 (dd, J = 18.0, 10.8 Hz, 1H, pyrazoline-H_4'), 4.18 (q, J = 7.2 Hz, 1H, CH), 6.11 (dd, J = 10.8, 3.2 Hz, 1H, pyrazoline-H_5), 7.00 (br s, 1H, Ar−H), 7.12 (d, J = 2.4 Hz, 1H, Ar−H), 7.24 (t, J = 4.2 Hz, 1H, Ar−H), 7.48 (d, J = 4.4 Hz, 1H, Ar−H), 7.69 (d, J = 2.8 Hz, 1H, Ar−H), 7.89 (d, J = 4.8 Hz, 1H, Ar−H). ^{13}C NMR (DMSO-d_6): δ 19.09, 44.06, 49.49, 59.80, 126.24, 126.46, 127.46, 128.96, 132.23, 132.92, 133.15, 142.56, 156.52, 175.99, 189.91. MS: m/z (%) 347 (M^+, 40.47). Anal. Calcd for $C_{15}H_{13}N_3OS_3$ (347.48): C, 51.85; H, 3.77; N, 12.09. Found: C, 51.94; H, 3.64; N, 12.22.

*4.1.4.2. 2-(4,5-Dihydro-5-(2,5-dimethoxyphenyl)-3-(thiophen-2-yl)pyrazol-1-yl)-5-methylthiazol-4(5H)-one (**7b**).* Buff crystals; mp 138−140 °C; yield: 85%. IR (cm^{-1}): 1728 (C═O), 1600 (C═N). ^{1}H NMR (DMSO-d_6): δ 1.47 (d, J = 7.6 Hz, 3H, CH_3), 3.25 (dd, J = 18.0, 4.0 Hz, 1H, pyrazoline-H_4), 3.66 (s, 3H, OCH_3), 3.76 (s, 3H, OCH_3), 4.02 (dd, J = 16.6, 11.4 Hz, 1H, pyrazoline-H_4'), 4.16 (q, J = 8.0 Hz, 1H, CH), 5.81 (dd, J = 11.2, 4.0 Hz, 1H, pyrazoline-H_5), 6.45 (br s, 1H, Ar−H), 6.87 (d, J = 7.2 Hz, 1H, Ar−H), 7.00 (d, J = 8.4 Hz, 1H, Ar−H), 7.20 (s, 1H, Ar−H), 7.59 (br s, 1H, Ar−H), 7.85 (d, J = 4.4 Hz, 1H, Ar−H). MS: m/z (%) 401 (M^+, 10.34). Anal. Calcd for $C_{19}H_{19}N_3O_3S_2$ (401.50): C, 56.84; H, 4.77; N, 10.47. Found: C, 56.72; H, 4.89; N, 10.58.

4.1.5. General Procedure for the Synthesis of Derivatives ***8a−d***. To a mixture of pyrazole-1-carbothioamides **2a,b** (0.01 mol), ethyl bromoacetate (1.67 mL, 0.01 mol), and the appropriate aldehyde, namely, 4-methoxybenzaldehyde or 2,5-dimethoxy benzaldehyde (0.01 mol), in glacial acetic acid (30 mL), a catalytic amount of anhydrous sodium acetate (1.64 g, 0.02 mol) was added and the reaction mixture was refluxed for 3−5 h; then, after the solution was cooled, it was poured into cold water. The solid formed was collected by filtration, dried, and crystallized from acetic acid to give the title compounds **8a−d**.

*4.1.5.1. 5-(4-Methoxybenzylidene)-2-(4,5-dihydro-3,5-di-(thiophen-2-yl)pyrazol-1-yl)thiazol-4(5H)-one (**8a**).* Brown crystals; mp 244−246 °C; yield: 77%. IR (cm^{-1}): 1695 (C═O), 1602 (C═N). ^{1}H NMR (DMSO-d_6): δ 3.68 (dd, J = 18.0, 3.2 Hz, 1H, pyrazoline-H_4), 3.84 (s, 3H, OCH_3), 4.13 (dd, J = 18.2, 11.0 Hz, 1H, pyrazoline-H_4'), 6.22 (dd, J = 10.6, 3.0 Hz, 1H, pyrazoline-H_5), 7.02 (t, J = 2.6 Hz, 1H, Ar−H), 7.12 (d, J = 8.8 Hz, 2H, Ar−H), 7.18 (d, J = 3.2 Hz, 1H, Ar−H), 7.27 (t, J = 4.4 Hz, 1H, Ar−H), 7.50 (d, J = 4.8 Hz, 1H, Ar−H), 7.61 (d, J = 8.4 Hz, 2H, Ar−H), 7.65 (s, 1H, ═CH), 7.74 (d, J = 3.2 Hz, 1H, Ar−H), 7.94 (d, J = 4.8 Hz, 1H, Ar−H). MS: m/z (%) 451 (M^+, 27.12). Anal. Calcd for $C_{22}H_{17}N_3O_2S_3$ (451.58): C, 58.51; H, 3.79; N, 9.31. Found: C, 58.63; H, 3.90; N, 9.44.

*4.1.5.2. 5-(4-Methoxybenzylidene)-2-(4,5-dihydro-5-(2,5-dimethoxyphenyl)-3-(thiophen-2-yl)pyrazol-1-yl)thiazol-4(5H)-one (**8b**).* Brown crystals; mp 173−175 °C; yield: 75%. IR (cm^{-1}): 1698 (C═O), 1605 (C═N). ^{1}H NMR (DMSO-d_6): δ 2.95 (dd, J = 17.4, 4.6 Hz, 1H, pyrazoline-H_4), 3.66 (s, 3H, OCH_3), 3.76 (s, 3H, OCH_3), 3.84 (s, 3H, OCH_3), 4.08 (dd, J = 18.0, 11.2 Hz, 1H, pyrazoline-H_4'), 5.91 (dd, J = 11.2, 4.0 Hz, 1H, pyrazoline-H_5), 6.55 (d, J = 2.8 Hz, 1H, Ar−H), 6.88 (d, J = 8.8 Hz, 1H, Ar−H), 7.02 (s, 1H, Ar−H), 7.12 (d, J = 8.4 Hz, 2H, Ar−H), 7.23 (t, J = 4.2 Hz, 1H, Ar−H), 7.62 (d, J = 8.8 Hz, 2H, Ar−H), 7.65 (s, 1H, ═CH), 7.87 (d, J = 8.8 Hz, 1H, Ar−H), 7.90 (d, J = 4.8 Hz, 1H, Ar−H). MS: m/z (%) 505 (M^+, 9.27). Anal. Calcd for $C_{26}H_{23}N_3O_4S_2$ (505.61): C, 61.76; H, 4.59; N, 8.31. Found: C, 61.84; H, 4.80; N, 8.40.

*4.1.5.3. 5-(2,5-Dimethoxybenzylidene)-2-(4,5-dihydro-3,5-di(thiophen-2-yl)pyrazol-1-yl)thiazol-4(5H)-one (**8c**).* Brown crystals; mp 220−222 °C; yield: 72%. IR (cm^{-1}): 1675 (C═O), 1600 (C═N). ^{1}H NMR (DMSO-d_6): δ 3.68 (dd, J = 18.0, 3.2 Hz, 1H, pyrazoline-H_4), 3.80 (s, 3H, OCH_3), 3.84 (s, 3H, OCH_3), 4.13 (dd, J = 18.0, 10.8 Hz, 1H, pyrazoline-H_4'), 6.22 (dd, J = 10.8, 3.2 Hz, 1H, pyrazoline-H_5), 7.01−7.09 (m, 4H, Ar−H), 7.19 (d, J = 3.2 Hz, 1H, Ar−H), 7.26 (t, J = 4.2 Hz, 1H, Ar−H), 7.50 (d, J = 5.2 Hz, 1H, Ar−H), 7.75 (d, J = 3.2 Hz, 1H, Ar−H), 7.86 (s, 1H, ═CH), 7.93 (d, J = 5.2 Hz, 1H, Ar−H). ^{13}C NMR (DMSO-d_6): δ 44.21, 56.04, 56.60, 59.96,

https://doi.org/10.1021/acsomega.3c04736
ACS Omega 2023, 8, 39250−39268

113.37, 114.25, 116.81, 123.56, 126.02, 126.68, 127.51, 128.85, 129.08, 132.63, 132.67, 133.59, 142.15, 152.76, 153.59, 157.39, 170.45, 179.34. MS: m/z (%) 481 (M^+, 9.45). Anal. Calcd for $C_{23}H_{19}N_3O_3S_3$ (481.61): C, 57.36; H, 3.98; N, 8.72. Found: C, 57.30; H, 3.90; N, 8.90.

*4.1.5.4. 5-(2,5-Dimethoxybenzylidene)-2-(4,5-dihydro-5-(2,5-dimethoxyphenyl)-3-(thiophen-2-yl)pyrazol-1-yl)-thiazol-4(5H)-one (**8d**).* Yellow crystals; mp 101−103 °C; yield: 76%. IR (cm^{-1}): 1698 (C═O), 1610 (C═N). ^1H NMR (DMSO-d_6): δ 3.06 (dd, J = 17.6, 5.2 Hz, 1H, pyrazoline-H_4), 3.67 (s, 3H, OCH_3), 3.76 (s, 3H, OCH_3), 3.81 (s, 3H, OCH_3), 3.84 (s, 3H, OCH_3), 4.08 (dd, J = 17.8, 11.4 Hz, 1H, pyrazoline-H_4'), 5.90 (dd, J = 11.4, 4.2 Hz, 1H, pyrazoline-H_5), 6.55 (d, J = 2.8 Hz, 1H, Ar−H), 6.88 (d, J = 8.8 Hz, 1H, Ar−H), 7.02−7.09 (m, 4H, Ar−H), 7.21 (d, J = 8.8 Hz, 1H, Ar−H), 7.65 (d, J = 3.2 Hz, 1H, Ar−H), 7.83 (s, 1H, ═CH), 7.89 (d, J = 4.8 Hz, 1H, Ar−H). MS: m/z (%) 535 (M^+, 16.19). Anal. Calcd for $C_{27}H_{25}N_3O_5S_2$ (535.63): C, 60.54; H, 4.70; N, 7.84. Found: C, 60.38; H, 4.85; N, 7.93.

*4.1.6. General Procedure for the Synthesis of Derivatives **9a,b**.* To a mixture of pyrazole-1-carbothioamides **2a,b** (0.01 mol), ethyl bromoacetate (1.67 mL, 0.01 mol), and isatin (1.47 g, 0.01 mol) in glacial acetic acid (30 mL), a catalytic amount of anhydrous sodium acetate (1.64 g, 0.02 mol) was added, and the reaction mixture was refluxed for 3−5 h; then after the solution was cooled, it was poured into cold water. The solid formed was collected by filtration, dried, and crystallized from acetic acid to give the title compounds **9a,b**.

*4.1.6.1. 3-(2-(4,5-Dihydro-3,5-di(thiophen-2-yl)pyrazol-1-yl)-4-oxothiazol-5(4H)-ylidene)indolin-2-one (**9a**).* Orange crystals; mp 284−286 °C; yield: 75%. IR (cm^{-1}): 3198 (NH), 1728 (C═O), 1695 (C═O), 1598 (C═N). ^1H NMR (DMSO-d_6): δ 3.70 (dd, J = 18.2, 3.4 Hz, 1H, pyrazoline-H_4), 4.14 (dd, J = 18.0, 10.8 Hz, 1H, pyrazoline-H_4'), 6.27 (dd, J = 10.4, 3.2 Hz, 1H, pyrazoline-H_5), 6.93 (d, J = 7.6 Hz, 1H, Ar−H), 7.02 (t, J = 4.4 Hz, 1H, Ar−H), 7.06 (t, J = 8.0 Hz, 1H, Ar−H), 7.20 (d, J = 2.8 Hz, 1H, Ar−H), 7.28 (t, J = 4.4 Hz, 1H, Ar−H), 7.36 (t, J = 7.6 Hz, 1H, Ar−H),7.50 (d, J = 5.2 Hz, 1H, Ar−H), 7.77 (d, J = 4.0 Hz, 1H, Ar−H), 7.97 (d, J = 5.2 Hz, 1H, Ar−H), 8.93 (d, J = 8.0 Hz, 1H, Ar−H), 11.17 (s, 1H, NH, exchangeable with D_2O). ^{13}C NMR (DMSO-d_6): δ 44.07, 60.03, 110.66, 120.81, 122.35, 126.67, 126.71, 127.52, 128.51, 129.13, 132.32, 132.66, 132.69, 132.90, 133.87, 137.15, 142.09, 143.69, 158.08, 169.44, 173.13, 179.33. MS: m/z (%) 462 (M^+, 23.71). Anal. Calcd for $C_{22}H_{14}N_4O_2S_3$ (462.57): C, 57.12; H, 3.05; N, 12.11. Found: C, 57.33; H, 3.11; N, 12.22.

*4.1.6.2. 3-(2-(4,5-Dihydro-5-(2,5-dimethoxyphenyl)-3-(thiophen-2-yl)pyrazol-1-yl)-4-oxothiazol-5(4H)-ylidene)-indolin-2-one (**9b**).* Orange crystals; mp 190−192 °C; yield: 70%. IR (cm^{-1}): 3170 (NH), 1725 (C═O), 1676 (C═O), 1600 (C═N). ^1H NMR (DMSO-d_6): δ 3.25 (dd, J = 18.0, 4.0 Hz, 1H, pyrazoline-H_4), 3.66 (s, 3H, OCH_3), 3.76 (s, 3H, OCH_3), 4.03 (dd, J = 17.8, 11.4 Hz, 1H, pyrazoline-H_4'), 5.80 (dd, J = 11.2, 4.0 Hz, 1H, pyrazoline-H_5), 6.45 (d, J = 2.8 Hz, 1H, Ar−H), 6.83 (d, J = 8.8 Hz, 1H, Ar−H), 6.92 (d, J = 7.6 Hz, 1H, Ar−H), 7.00 (s, 1H, Ar−H), 7.10 (t, J = 8.0 Hz, 1H, Ar−H), 7.23 (d, J = 8.8 Hz, 1H, Ar−H), 7.40 (t, J = 7.6 Hz, 1H, Ar−H), 7.61 (d, J = 3.6 Hz, 1H, Ar−H), 7.85 (d, J = 5.2 Hz, 1H, Ar−H), 8.79 (d, J = 8.0 Hz, 1H, Ar−H), 11.20 (s, 1H, NH, exchangeable with D_2O). MS: m/z (%) 516 (M^+, 7.64). Anal. Calcd for $C_{26}H_{20}N_4O_4S_2$ (516.59): C, 60.45; H, 3.90; N, 10.85. Found: C, 60.51; H, 3.78; N, 10.97.

*4.1.7. General Procedure for the Synthesis of Derivatives **10a,b**.* A mixture of pyrimidin-2-thione derivatives **2a**, **2b** (0.01 mol), 3-bromopropanoic acid (1.54 g, 0.01 mol), and anhydrous sodium acetate (1.64 g, 0.02 mol) in glacial acetic acid (20 mL) was refluxed for 6 h. The reaction mixture was cooled and poured into cold water, and the solid formed was collected and crystallized from acetic acid to give compounds **10a,b**.

*4.1.7.1. 5,6-Dihydro-2-(4,5-dihydro-3,5-di(thiophen-2-yl)-pyrazol-1-yl)-1,3-thiazin-4-one (**10a**).* Brown crystals; mp 149−151 °C; yield: 73%. IR (cm^{-1}): 1692 (C═O), 1590 (C═N). ^1H NMR (DMSO-d_6): δ 3.18−3.23 (m, 4H, $2CH_2$), 3.53 (dd, J = 18.0, 2.8 Hz, 1H, pyrazoline-H_4), 3.81 (dd, J = 17.6, 11.2 Hz, 1H, pyrazoline-H_4'), 5.84 (dd, J = 11.4, 3.8 Hz, 1H, pyrazoline-H_5), 6.94 (d, J = 3.6 Hz, 1H, Ar−H), 7.02 (d, J = 3.2 Hz, 1H, Ar−H), 7.16 (d, J = 3.6 Hz, 1H, Ar−H), 7.40 (d, J = 4.8 Hz, 1H, Ar−H), 7.52 (d, J = 3.6 Hz, 1H, Ar−H), 7.75 (d, J = 5.2 Hz, 1H, Ar−H). MS: m/z (%) 347 (M^+, 34.08). Anal. Calcd for $C_{15}H_{13}N_3OS_3$ (347.48): C, 51.85; H, 3.77; N, 12.09. Found: C, 51.99; H, 3.68; N, 12.17.

*4.1.7.2. 5,6-Dihydro-2-(4,5-dihydro-5-(2,5-dimethoxy-phenyl)-3-(thiophen-2-yl)pyrazol-1-yl)-1,3-thiazin-4-one (**10b**).* Brown crystals; mp: 168−170 °C; yield: 69%. IR (cm^{-1}): 1690 (C═O), 1595 (C═N). ^1H NMR (DMSO-d_6): δ 2.95 (dd, J = 17.6, 4.4 Hz, 1H, pyrazoline-H_4), 3.18−3.25 (m, 4H, 2 CH_2), 3.77 (s, 3H, OCH_3), 3.79 (s, 3H, OCH_3), 3.91 (dd, J = 18.0, 10.8 Hz, 1H, pyrazoline-H_4'), 5.60 (dd, J = 11.6, 4.4 Hz, 1H, pyrazoline-H_5), 6.36 (d, J = 2.8 Hz, 1H, Ar−H), 6.80 (d, J = 8.8 Hz, 1H, Ar−H), 6.96 (s, 1H, Ar−H), 7.12 (d, J = 8.8 Hz, 1H, Ar−H), 7.42 (d, J = 3.2 Hz, 1H, Ar−H), 7.71 (d, J = 4.8 Hz, 1H, Ar−H). MS: m/z (%) 401 (M^+, 8.45). Anal. Calcd for $C_{19}H_{19}N_3O_3S_2$ (401.5): C, 56.84; H, 4.77; N, 10.47. Found: C, 56.95; H, 4.66; N, 10.69.

4.2. Antimicrobial Activity. *4.2.1. Antibacterial and Antifungal Activity.* The antimicrobial property was achieved using broth microdilution assay. The minimum inhibitory concentrations (MICs) were determined in 96-well plates (the experiment is displayed in Supporting Information).

4.2.2. Antituberculosis Activity. Antituberculosis activity was estimated using the Microplate alamar blue assay (MABA) method. MICs of the examined compounds were calculated using isoniazid as a reference drug against *M. tuberculosis* (RCMB 010126) that was gotten from the Regional Center for Mycology and Biotechnology (RCMB), Al-Azhar University, Cairo, Egypt (the experiment is displayed in Supporting Information).

4.2.3. In Vitro Assay for Mtb DHFR. The experiment is displayed in Supporting Information.

4.3. Biodistribution Study of Compound 6b. Compound **6b** was further selected for biodistribution study via radiolabeling with ^{131}I.

*4.3.1. Radiolabeling of Compound **6b**.* The radioiodination process of compound **6b** was achieved using oxidizing agents, Chloramine-T. Briefly, adequate quantity of the compound **6b** was dissolved in DMSO 10 μL of sodium ^{131}I iodide (50 μCi) was added to this solution, followed by adequate quantity of Chloramine-T solution in 0.05 M phosphate buffer (pH 7.4). After adjusting the mixture pH to be the optimum one (pH 7), the resulting admixture was incubated at several temperatures (25, 40, 60, 80, and 100 °C) for several time periods (10, 15, 30, 45, and 60 min). The radiolabeling efficiency (RE) of labeled compound was

https://doi.org/10.1021/acsomega.3c04736
ACS Omega 2023, 8, 39250−39268

checked by TLC chromatographic method and paper electrophoresis.

The influence of various amounts of both compound **6b** (50, 100,150, 200, and 250 μg) and Chloramine-T (50, 100, 150, 200, and 250 μg) were investigated to obtain the optimum amounts for maximum radiolabeling efficiency. Each trial was repeated thrice (n = 3), and the data was expressed as mean ± SD. Certainly,% RE was calculated from eq 1.

$$\% \text{ RE} = \frac{\text{radio activity of radiolabeled compound}}{\text{total activity}} \times 100 \quad (1)$$

4.3.2. In Vitro Stability. Post radiolabeling, the same procedures which used for % RE determination were conducted to investigate in vitro stability of the optimum radiolabeled compound and the data was recorded at predetermined time intervals for up to 36 h.

4.3.3. Infection Induction in Mice. Swiss Albino male mice, 20−25 g were used. Infection was induced by inoculation of 0.1 mL of *P. aeruginosa* (1.2 × 109 cfu/mL) in the left upper thigh muscle (left as target, right as control).[53]

*4.3.4. Tissue Distribution Study of Radiolabeled Compound **6b** in Healthy Mice and Infected Models.* For inspecting the biological behavior of radiolabeled compound **6b** in vivo, two groups of mice (Swiss Albino mice weighing 20−25 g) each comprise 12 mice; 1 is healthy and the others are infected models (n = 3 for each set of experiment).

In this study, 0.2 mL (15.6 MBq) of radiolabeled compound **6b** dispersed in normal saline (0.9% NaCl) was intravenously injected to the tail vein of each mouse. The mice were sacrificed at 30 min, 60 min, 2 h, and 4 h time points. Various body organs such as the heart, liver, kidney, lung, heart, and right and left thigh muscles (normal and infected) were isolated and washed with saline and weighed and counted for their radioactivity content using gamma counter. The blood sample was collected by cardiac-puncture and radioactivity in blood, muscles and bones calculated as 7, 40, and 10% of total animal body-weight, respectively.[54] The data of tissue distribution study were represented as % injected dose/gram organ (% ID/g).

*4.3.5. Target to Nontarget Uptake Ratio of Radiolabeled Compound **6b**.* Target/non-target ratios are the key factors to evaluate the selectivity and targeting of 131I-**6b** compound to the infection.[55]

Radiolabeled compound **6b** must be localized in the infected muscle (the target) in a high ratio when compared to the normal muscle (the nontarget). In this regard, the infected/normal-muscle (T/NT) ratio was determined using eq 2.

$$\text{T/NT} = \frac{\text{\% ID/g of infected muscle}}{\text{\% ID/g of normal muscle}} \quad (2)$$

4.4. Molecular Docking. The molecular docking simulation of the in vitro inhibitory thiophenyl-pyrazolyl-thiazole hybrids **4c**, **6b**, **8b**, **9b**, and **10b** against *M. tuberculosis* dihydrofolate reductase enzyme was applied using the Molecular Operating Environment software (MOE-Dock) version 2014.0901.[47,48] The cocrystallized structure of *M. tuberculosis* DHFR complexed with its original ligand, trimethoprim, was downloaded from the protein data bank (PDB code: 1DG5).[49] Initially, the original ligands were redocked into the active binding site of *M. tuberculosis* DHFR to estimate the root-mean-square deviation value. After that, the docking studies of the newly synthesized thiophenyl-pyrazolyl-thiazole hybrids were assessed regarding to the previously cited procedure.[56]

4.5. ADMET Prediction Study. The promising thiophenyl-pyrazolyl-thiazole hybrids **4c**, **6b**, and **10b** were further examined for their anticipated physicochemical and pharmacokinetic features utilizing the free available web tool, SwissADME, in accordance with the outlined procedure.[50,51]

Additionally, their toxicity was calculated using the online server admetSAR 1.0 (http://lmmd.ecust.edu.cn/admetsar1),[57] which forecasts the values of the studied molecule's carcinogenicity, the acute oral toxicity, Ames toxicity, and inhibition of the human Ether-a-go-go-related gene.

■ ASSOCIATED CONTENT

Supporting Information

The Supporting Information is available free of charge at https://pubs.acs.org/doi/10.1021/acsomega.3c04736.

Pharmacokinetic features, molecular modeling study on DHFR (3D binding poses), ^{1}H NMR, and ^{13}C NMR spectra of the new compounds, antibacterial, antifungal, and antituberculosis assay, and in vitro assay for *Mtb* DHFR (PDF)

■ AUTHOR INFORMATION

Corresponding Author

Dina H. Dawood − *Chemistry of Natural and Microbial Products Department, Pharmaceutical and Drug Industries Research Institute, National Research Centre, Giza 12622, Egypt*; orcid.org/0000-0001-6537-5979; Email: dinanrc@yahoo.com, dh.dawood@nrc.sci.eg

Authors

Manal M. Sayed − *Labeled Compounds Department, Hot Labs.center, Egyptian Atomic Energy Authority (EAEA), 13759 Cairo, Egypt*

Sally T. K. Tohamy − *Department of Microbiology and Immunology, Faculty of Pharmacy (Girls), Al-Azhar University, Cairo 11754, Egypt*

Eman S. Nossier − *Department of Pharmaceutical Medicinal Chemistry and Drug Design, Faculty of Pharmacy (Girls), Al-Azhar University, Cairo 11754, Egypt; The National Committee of Drugs, Academy of Scientific Research and Technology, Cairo 11516, Egypt*

Complete contact information is available at: https://pubs.acs.org/10.1021/acsomega.3c04736

Funding

This research did not receive any specific grant from funding agencies in the public, commercial, or not-for-profit sectors.

Notes

All experiments were approved by the Medical Research Ethical Committee of the National Research Centre (81112012023).

The authors declare no competing financial interest.

■ ACKNOWLEDGMENTS

The authors thank the National Research Centre for supporting this work.

REFERENCES

(1) Lomazzi, M.; Moore, M.; Johnson, A.; Balasegaram, M.; Borisch, B. Antimicrobial resistance-moving forward? *BMC Public Health* **2019**, *19*, 858.

(2) Chokshi, A.; Sifri, Z.; Cennimo, D.; Horng, H. Global contributors to antibiotic resistance. *J. Global Infect. Dis.* **2019**, *11*, 36−42.

(3) Isturiz, R. E. Optimizing antimicrobial prescribing. *Int. J. Antimicrob. Agents* **2010**, *36*, S19−S22.

(4) De Kraker, M. E. A.; Stewardson, A. J.; Harbarth, S. Will 10 million people die a year due to antimicrobial resistance by 2050? *PLoS Med.* **2016**, *13*, No. e1002184.

(5) He, J.; Qiao, W.; An, Q.; Yang, T.; Luo, Y. Dihydrofolate reductase inhibitors for use as antimicrobial agents. *Eur. J. Med. Chem.* **2020**, *195*, 112268.

(6) Lele, A. C.; Raju, A.; Ray, M. K.; Rajan, M. G. R.; Degani, M. S. Design and Synthesis of Diaminotriazines as Anti-Tuberculosis DHFR Inhibitors. *Curr. Res. Drug Discov.* **2014**, *1* (2), 45−50.

(7) Hong, W.; Wang, Y.; Chang, Z.; Yang, Y.; Pu, J.; Sun, T.; Kaur, S.; Sacchettini, J. C.; Jung, H.; Lin Wong, W.; Fah Yap, L.; Fong Ngeow, Y.; Paterson, I. C.; Wang, H. The identification of novel Mycobacterium tuberculosis DHFR inhibitors and the investigation of their binding preferences by using molecular modelling. *Sci. Rep.* **2015**, *5*, 15328.

(8) Hajian, B.; Scocchera, E.; Shoen, C.; Krucinska, J.; Viswanathan, K.; G-Dayanandan, N.; Erlandsen, H.; Estrada, A.; Mikusova, K.; Kordulakova, J.; Cynamon, M.; Wright, D. Drugging the Folate Pathway in Mycobacterium tuberculosis: The Role of Multi-targeting Agent. *Cell Chem. Biol.* **2019**, *26*, 781−791.

(9) He, J.; Li, C.; Hu, W.; Li, C.; Liu, S.; Sui, J.; Zhang, T.; Sun, Q.; Luo, Y. Identification of selective mtbDHFR inhibitors by virtual screening and experimental approaches. *Chem. Biol. Drug Des.* **2022**, *100*, 1005−1016.

(10) Scocchera, E.; Reeve, S. M.; Keshipeddy, S.; Lombardo, M. N.; Hajian, B.; Sochia, A. E.; Alverson, J. B.; Priestley, N. D.; Anderson, A. C.; Wright, D. L. Charged nonclassical antifolates with activity against Gram-positive and Gram-negative pathogens. *ACS Med. Chem. Lett.* **2016**, *7*, 692−696.

(11) Blakley, R. L. Dihydrofolate reductase. In *Folates and Pterines*; Blakley, R. L., Benkovic, S. J., Eds.; Wiley: New York, 1984, pp 191−253.

(12) Blakley, R. L. Eukaryotic dihydrofolate reductase. *Adv. Enzymol. Relat. Areas Mol. Biol.* **1995**, *70*, 23−102.

(13) Rashid, N.; Thapliyal, C.; Chattopadhyay, P. C. Dihydrofolate reductase as a versatile drug target in healthcare. *J. Protein Proteonomics* **2016**, *7*, 247−257.

(14) Ashalatha, B. V.; Narayana, B.; Vijaya Raj, K.; Suchetha Kumari, N. Synthesis of some new bioactive 3-amino-2-mercapto-5,6,7,8-tetrahydro[1]benzothieno[2,3-d]pyrimidin-4(3H)-one derivatives. *Eur. J. Med. Chem.* **2007**, *42*, 719−728.

(15) Kotaiah, Y.; Harikrishna, N.; Nagaraju, K.; Venkata Rao, C. Synthesis and antioxidant activity of 1,3,4-oxadiazole tagged thieno-[2,3-d]pyrimidine derivatives. *Eur. J. Med. Chem.* **2012**, *58*, 340−345.

(16) Malani, K.; Thakkar, S. S.; Thakur, M. C.; Ray, A.; Doshi, H. Synthesis, characterization and in silico designing of diethyl-3-methyl-5-(6-methyl-2-thioxo-4-phenyl-1,2,3,4-tetrahydro- pyrimidine-5-carboxamido) thiophene-2,4-dicarboxylate derivative as anti-proliferative and anti-microbial agents. *Bioorg. Chem.* **2016**, *68*, 265−274.

(17) Dawood, D. H.; Nossier, E. S.; Abd elhameed, M. F.; Asaad, G. F.; Abd El-Rahman, S. S. Design, synthesis, anti-inflammatory evaluation and molecular docking of novel thiophen-2-ylmethylene-based derivatives as potential TNF-α production inhibitors. *Bioorg. Chem.* **2022**, *122*, 105726.

(18) Pinto, E.; Queiroz, M. J. R. P.; Vale-Silva, L. A.; Oliveira, J. F.; Begouin, A.; Begouin, J. M.; Kirsch, G. Antifungal activity of synthetic di(hetero)arylamines based on the benzo[b]thiophene moiety. *Bioorg. Med. Chem.* **2008**, *16*, 8172−8177.

(19) Saravanan, J.; Mohan, S.; Roy, J. J. Synthesis of some 3-substituted amino-4,5-tetramethylene thieno[2,3-d] [1,2,3]-triazin-4(3H)-ones as potential antimicrobial agents. *Eur. J. Med. Chem.* **2010**, *45*, 4365−4369.

(20) Hafez, H. N.; Hussein, H. A. R.; El-Gazzar, A. R. B. Synthesis of substituted thieno[2,3-d]pyrimidine-2,4-dithiones and their S-glycoside analogues as potential antiviral and antibacterial agents. *Eur. J. Med. Chem.* **2010**, *45*, 4026−4034.

(21) Gouda, M. A.; Berghot, M. A.; Abd El-Ghani, G. E.; Khalil, A. M. Synthesis and antimicrobial activities of some new thiazole and pyrazole derivatives based on 4,5,6,7-tetrahydrobenzothiophene moiety. *Eur. J. Med. Chem.* **2010**, *45*, 1338−1345.

(22) Baldo, B. A.; Phan, N. H. *Drug Allergy: Clinical aspects, diagnosis, mechanism, Structure-Activity Relationship*; Springer NewYork Heidelberg Dordrecht: London, 2017; pp 134−162.

(23) Aly, H. M.; Saleh, N. M.; Elhady, H. A. Design and synthesis of some new thiophene, thienopyrimidine and thienothiadiazine derivatives of antipyrine as potential antimicrobial agents. *Eur. J. Med. Chem.* **2011**, *46*, 4566−4572.

(24) Asiri, A. M.; Khan, S. A. Synthesis and Anti-Bacterial Activities of a Bis-Chalcone Derived from Thiophene and Its Bis-Cyclized Products. *Molecules* **2011**, *16*, 523−531.

(25) Radini, I. A. M. Design, Synthesis, and Antimicrobial Evaluation of Novel Pyrazoles and Pyrazolyl 1,3,4-Thiadiazine Derivatives. *Molecules* **2018**, *23*, 2092.

(26) Parai, M. K.; Panda, G.; Chaturvedi, V.; Manju, Y. K.; Sinha, S. Thiophene containing triarylmethanes as antitubercular agents. *Bioorg. Med. Chem. Lett.* **2008**, *18*, 289−292.

(27) Meena, C. L.; Singh, P.; Shaliwal, R. P.; Kumar, V.; Kumar, A.; Tiwari, A. K.; Asthana, S.; Singh, R.; Mahajan, D. Synthesis and evaluation of thiophene based small molecules as potent inhibitors of Mycobacterium tuberculosis. *Eur. J. Med. Chem.* **2020**, *208*, 112772.

(28) Xu, Z.; Gao, C.; Ren, Q. C.; Song, X. F.; Feng, L. S.; Lv, Z. S. Recent advances of pyrazole-containing derivatives as anti-tubercular agents. *Eur. J. Med. Chem.* **2017**, *139*, 429−440.

(29) Gupta, V.; Kant, V. A Review on Biological Activity of Imidazole and Thiazole Moieties and their Derivatives. *Sci. Int.* **2013**, *1*, 253−260.

(30) Dawane, B. S.; Konda, S. G.; Shaikh, B. M.; Chobe, S. S.; Khandare, N. T.; Kamble, V. T.; Bhosale, R. B. Synthesis and in vitro antimicrobial activity of some new 1-thiazolyl-2- pyrazoline derivatives. *Synthesis* **2010**, *1*, 44−48.

(31) Borcea, A.-M.; Ionuţ, I.; Crişan, O.; Oniga, O. An Overview of the Synthesis and Antimicrobial, Antiprotozoal, and Antitumor Activity of Thiazole and Bisthiazole Derivatives. *Molecules* **2021**, *26*, 624.

(32) Ayati, A.; Emami, S.; Asadipour, A.; Shafiee, A.; Foroumadi, A. Recent applications of 1,3-thiazole core structure in the identification of new lead compounds and drug discovery. *Eur. J. Med. Chem.* **2015**, *97*, 699−718.

(33) Cuartas, V.; Robledo, S. M.; Vélez, I. D.; Crespo, M. P.; Sortino, M.; Zacchino, S.; Nogueras, M.; Cobo, J.; Upegui, Y.; Pineda, T.; Yepes, L.; Insuasty, B. New thiazolyl-pyrazoline derivatives bearing nitrogen mustard as potential antimicrobial and antiprotozoal agents. *Arch. Pharm.* **2020**, *353*, No. e1900351.

(34) Mansour, E.; Aboelnaga, A.; Nassar, E. M.; Elewa, S. I. A new series of thiazolyl pyrazoline derivatives linked to benzo[1,3]dioxole moiety: Synthesis and evaluation of antimicrobial and anti-proliferative activities. *Synth. Commun.* **2020**, *50*, 368−379.

(35) Bhandare, R. R.; S. Munikrishnappa, C.; Suresh Kumar, G.; Konidala, S. K.; Sigalapalli, D. K.; Vaishnav, Y.; Chinnam, S.; Yasin, H.; Al-karmalawy, A. A.; Shaik, A. B. Multistep synthesis and screening of heterocyclic tetrads containing furan, pyrazoline, thiazole and triazole (or oxadiazole) as antimicrobial and anticancer agents. *J. Saudi Chem. Soc.* **2022**, *26*, 101447.

(36) Altintop, M. D.; Ozdemir, A.; Turan-Zitouni, G.; Ilgin, S.; Atli, O.; Demirel, R.; Kaplancikli, Z. A. A novel series of thiazolyl−pyrazoline derivatives: Synthesis and evaluation of antifungal activity, cytotoxicity and genotoxicity. *Eur. J. Med. Chem.* **2015**, *92*, 342−352.

(37) Takate, S. J.; Shinde, A. D.; Karale, B. K.; Akolkar, H.; Nawale, L.; Sarkar, D.; Mhaske, P. C. Thiazolyl-pyrazole derivatives as

https://doi.org/10.1021/acsomega.3c04736
ACS Omega 2023, 8, 39250−39268

potential antimycobacterial agents. *Bioorg. Med. Chem. Lett.* **2019**, *29*, 1199−1202.
(38) Mohamed, H. A.; Ammar, Y. A.; Elhagali, G. A. M.; Eyada, H. A.; Aboul-Magd, D. S.; Ragab, A. In Vitro Antimicrobial Evaluation, Single-Point Resistance Study, and Radiosterilization of Novel Pyrazole Incorporating Thiazol-4-one/ Thiophene Derivatives as Dual DNA Gyrase and DHFR Inhibitors against MDR Pathogens. *ACS Omega* **2022**, *7*, 4970−4990.
(39) Alzahrani, A. Y.; Ammar, Y. A.; Abu-Elghait, M.; Salem, M. A.; Assiri, M. A.; Ali, T. E.; Ragab, A. Development of novel indolin-2-one derivative incorporating thiazole moiety as DHFR and quorum sensing inhibitors: Synthesis, antimicrobial, and antibiofilm activities with molecular modelling study. *Bioorg. Chem.* **2022**, *119*, 105571.
(40) Ibrahim, S. A.; Fayed, E. A.; Rizk, H. F.; Desouky, S. E.; Ragab, A. Hydrazonoyl bromide precursors as DHFR inhibitors for the synthesis of bis-thiazolyl pyrazole derivatives; antimicrobial activities, antibiofilm, and drug combination studies against MRSA. *Bioorg. Chem.* **2021**, *116*, 105339.
(41) Geskovski, N.; Kuzmanovska, S.; Simonoska Crcarevska, M.; Calis, S.; Dimchevska, S.; Petrusevska, M.; Zdravkovski, P.; Goracinova, K. Comparative biodistribution studies of technetium-99 m radiolabeled amphiphilic nanoparticles using three different reducing agents during the labeling procedure. *J. Labelled Compd. Radiopharm.* **2013**, *56* (14), 689−695.
(42) Banerjee, T.; Singh, A. K.; Sharma, R. K.; Maitra, A. N. Labeling efficiency and biodistribution of technetium-99m labeled nanoparticles: interference by colloidal tin oxide particles. *Int. J. Pharm.* **2005**, *289* (1−2), 189−195.
(43) Loudos, G.; Kagadis, G. C.; Psimadas, D. Current status and future perspectives of in vivo small animal imaging using radiolabeled nanoparticles. *Eur. J. Radiol.* **2011**, *78* (2), 287−295.
(44) Syam, Y. M.; Anwar, M. M.; Abd El-Karim, S. S.; Elseginy, S. A.; Essa, B. M.; Sakr, T. M. New quinoxaline compounds as DPP-4 inhibitors and hypoglycemics: design, synthesis, computational and bio-distribution studies. *RSC Adv.* **2021**, *11*, 36989−37010.
(45) Mohamed, K. O.; Nissan, Y. M.; El-Malah, A. A.; Ahmed, W. A.; Ibrahim, D. M.; Sakr, T. M.; Motaleb, M. A. Design, synthesis and biological evaluation of some novel sulfonamide derivatives as apoptosis inducers. *Eur. J. Med. Chem.* **2017**, *135*, 424−433.
(46) Durante, A. C. R.; Sobral, D.V.; Miranda, A. C.; de Almeida, É. V.; Fuscaldi, L. L.; de Barboza, M. R. F. F.; Malavolta, L. Comparative Study of Two Oxidizing Agents, Chloramine T and Iodo-Gen, for the Radiolabeling of β-CIT with Iodine-131: Relevance for Parkinson's Disease. *Pharmaceuticals* **2019**, *12* (1), 25.
(47) Amr, A. E. G. E.; Elsayed, E. A.; Al-Omar, M. A.; Badr Eldin, H. O.; Nossier, E. S.; Abdallah, M. M. Design, synthesis, anticancer evaluation and molecular modeling of novel estrogen derivatives. *Molecules* **2019**, *24* (3), 416.
(48) Othman, I. M.; Gad-Elkareem, M. A.; Amr, A. E. G. E.; Al-Omar, M. A.; Nossier, E. S.; Elsayed, E. A. Novel heterocyclic hybrids of pyrazole targeting dihydrofolate reductase: design, biological evaluation and in silico studies. *J. Enzyme Inhib. Med. Chem.* **2020**, *35* (1), 1491−1502.
(49) Li, R.; Sirawaraporn, R.; Chitnumsub, P.; Sirawaraporn, W.; Wooden, J.; Athappilly, F.; Turley, S.; Hol, W. G. Three-dimensional structure of M. tuberculosis dihydrofolate reductase reveals opportunities for the design of novel tuberculosis drugs. *J. Mol. Biol.* **2000**, *295* (2), 307−323.
(50) Mohi El-Deen, E. M.; Nossier, E. S.; Karam, E. A. New Quinazolin-4 (3 H)-one Derivatives Incorporating Hydrazone and Pyrazole Scaffolds as Antimicrobial Agents Targeting DNA Gyraze Enzyme. *Sci. Pharm.* **2022**, *90* (3), 52.
(51) Othman, I. M. M.; Alamshany, Z. M.; Tashkandi, N. Y.; Gad-Elkareem, M. A.; Abd El-Karim, S. S.; Nossier, E. S. Synthesis and biological evaluation of new derivatives of thieno-thiazole and dihydrothiazolo-thiazole scaffolds integrated with a pyrazoline nucleus as anticancer and multi-targeting kinase inhibitors. *RSC Adv.* **2022**, *12* (1), 561−577.
(52) Ozdemir, Z.; Kandilci, H. B.; Gumusel, B.; Calis, U.; Bilgin, A. A. Synthesis and studies on antidepressant and anticonvulsant activities of some 3-(2-thienyl) pyrazoline derivatives. *Arch. Pharm.* **2008**, *341*, 701−707.
(53) Vilche, M.; Reyes, A. L.; Vasilskis, E.; Oliver, P.; Balter, H.; Engler, H. ^{68}Ga-NOTA-UBI-29−41 as a PET Tracer for Detection of Bacterial Infection. *J. Nucl. Med.* **2016**, *57*, 622−627.
(54) Khater, S. I.; El-Sharawy, D. M.; El Refaye, M. S.; Farrag, N. S. Optimization and tissue distribution of [125I] iododomperidone as a radiotracer for D2-receptor imaging. *J. Radioanal. Nucl. Chem.* **2020**, *325* (2), 343−355.
(55) Farrag, N. S.; Shetta, A.; Mamdouh, W. Green tea essential oil encapsulated chitosan nanoparticles-based radiopharmaceutical as a new trend for solid tumor theranosis. *Int. J. Biol. Macromol.* **2021**, *186*, 811−819.
(56) Amr, A. E. G. E.; Abdel-Mageid, R. E.; El-Naggar, M.; Naglah, A. M.; Nossier, E. S.; Elsayed, E. A. Chiral Pyridine-3, 5-bis-(L-phenylalaninyl-L-leucinyl) Schiff Base Peptides as Potential Anti-cancer Agents: Design, Synthesis, and Molecular Docking Studies Targeting Lactate Dehydrogenase-A. *Molecules* **2020**, *25* (5), 1096.
(57) Guerraoui, A.; Goudjil, M.; Direm, A.; Guerraoui, A.; Şengün, İ. Y.; Parlak, C.; Djedouani, A.; Chelazzi, L.; Monti, F.; Lunedei, E.; Boumaza, A. A rhodanine derivative as a potential antibacterial and anticancer agent: Crystal structure, spectral characterization, DFT calculations, Hirshfeld surface analysis, in silico molecular docking and ADMET studies. *J. Mol. Struct.* **2023**, *1280*, 135025.

https://doi.org/10.1021/acsomega.3c04736
ACS Omega 2023, 8, 39250−39268